Elemental and Reactive Gaseous Mercury Deposition and Diurnal Cycles over Terrestrial Environments

by

Anastasia F. Maheras

Submitted to the Department of Earth, Atmospheric and Planetary Sciences

in Partial Fulfillment of the Requirements for the Degree of

Bachelor of Science in Earth, Atmospheric and Planetary Sciences

at the Massachusetts Institute of Technology

June 2011

Author Signature redacted
Department of Earth, Atmospheric and Planetary Sciences
May 6, 2011

Certified by Signature redacted
Noelle E. Selin
Thesis Supervisor

Accepted by Signature redacted
Samuel Bowring
Chair, Committee on Undergraduate Program

Elemental and Reactive Gaseous Mercury Deposition and Diurnal Cycles over Terrestrial Environments

Anastasia F. Maheras

Submitted to the
Department of Earth, Atmospheric, and Planetary Sciences
May 6, 2011

Advisor

Noelle E. Selin, PhD
Massachusetts Institute of Technology

ABSTRACT

The atmospheric component of the global biogeochemical mercury cycle was studied to determine the mechanisms behind diurnal trends and amplitudes in elemental and reactive gaseous mercury concentrations over terrestrial environments. This analysis was done using the 3D GEOS-Chem chemical transport model and the creation of a simple one-box model. Mercury is a significant neurotoxin for humans and other species that has been addressed in the policy realm on both national and international levels. Being able to model atmospheric mercury processes correctly is an important part of regulation and policy drafting. GEOS-Chem model results were compared with *Weiss-Penzias et al.* [2009] measurements for three Nevada, USA sites. The magnitude of elemental mercury concentrations differed by 0.07-0.2 ng/m^3, with GEOS-Chem underestimating concentrations due to an under-representation of mercury emissions at naturally enriched sites. The amplitude of reactive gaseous mercury diurnal variations differed by a factor of 3-4, with GEOS-Chem underestimating the diurnal trend. Based on the diurnal nature of this error, it is hypothesized that GEOS-Chem under represents the magnitude of elemental mercury emissions, the amount of oxidation occurring in the atmosphere, and the scale of entrainment from the free troposphere.

ACKNOWLEDGMENTS

I would like to thank the following people for their help throughout the thesis process:

Noelle Selin for her help, commitment, and the enormous amount of time she gave me during the research and writing process.

My friends and family for giving me moral support during the year and my parents for inspiring me to pursue science.

TABLE OF CONTENTS

LIST OF FIGURES

LIST OF TABLES

1. INTRODUCTION

The growing concern over mercury's effect on the health and development of human populations has spurred research in the area of the global biogeochemical mercury cycle. Although most human exposure to mercury occurs from mercury that is incorporated into fish tissue, the majority of mercury transport actually occurs in the atmosphere. The purpose of this study is to determine and quantify the mechanisms controlling elemental and reactive gaseous mercury deposition over land over long-term and daily time scales.

Given the threat posed to both human and animal populations by rising mercury levels, governments across the world are keen to address the regulation and control of mercury emissions. Mercury occurs naturally in the environment. Much like carbon, it cycles through various reservoirs, including the earth, atmosphere, and oceans. Also, much like carbon, mercury levels are increasing due to anthropogenic activity, including manufacturing and fossil fuel burning [*Environmental Protection Agency (EPA),* 1997]. Rising levels of mercury are a concern because of the element's toxic properties [*Environmental Protection Agency (EPA),* 1997]. Methylmercury (CH_3Hg^+) is an especially hazardous mercury compound because it acts as a toxin; in this form, mercury is detrimental to neural pathways, especially in developing children [*Mergler et al.,* 2007]. The

effects of methylmercury are not limited to humans; wildlife is also negatively affected by rising mercury levels [*Wolfe et al.,* 1998; *Vo et al.,* 2011]. Methylmercury is bioaccumulated, thus posing a threat to animals farther up the food chain and potentially being more hazardous to humans than other species [*Mergler et al.,* 2007]. Scientific consensus regarding how mercury interacts chemically with the environment would be useful in helping draft successful, efficient policies to mitigate mercury exposure.

Mercury can interact with its environment in different ways depending on its location in the biogeochemical cycle, which consists of reservoirs of mercury as well as various types of transport between reservoirs. Major reservoirs of mercury include the atmosphere, ocean, and land. The latter reservoir includes soils and plants and is often referred to as the terrestrial reservoir. Mercury moves between these reservoirs at different rates and through different processes, including emissions from volcanism, runoff, and deposition (see Figure 1, page 11) [*Selin,* 2009]. These rates have been altered as the result of anthropogenic activities, such as fossil fuel burning, which has increased the amount of mercury being released to the atmosphere [*Mason et al.,* 1994; *Environmental Protection Agency (EPA),* 1997].

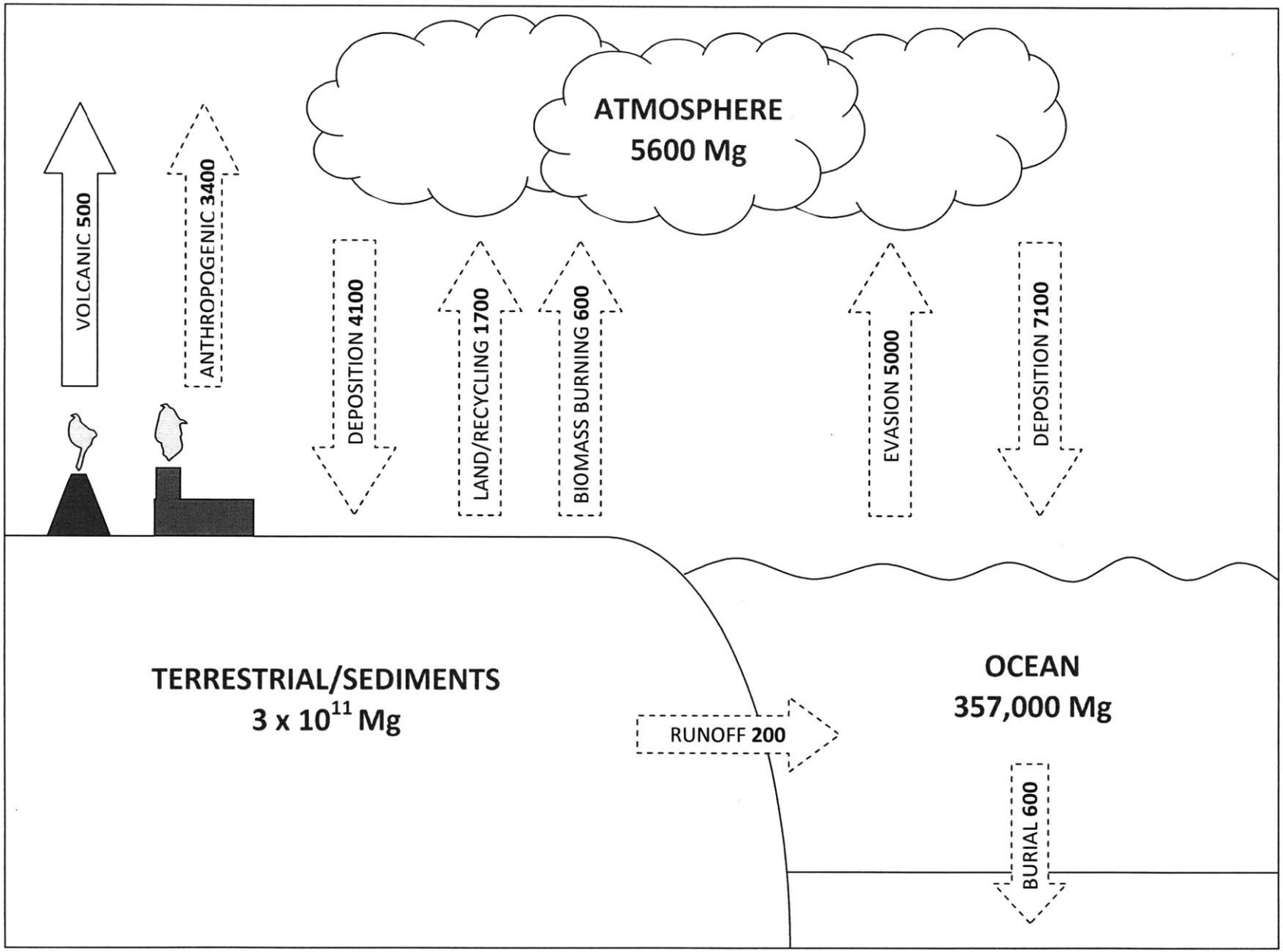

Figure 1. Simplified Global Biogeochemical Mercury Cycle. Reservoirs are in bold with inventories in Mg. Fluxes are depicted by arrow with rates in Mg a^{-1}. Completely natural fluxes are depicted by solid arrows. Anthropogenic/anthropogenically enhanced fluxes are depicted by dashed arrows. Note that this figure does not distinguish between different species of mercury. Also note that fluxes that are anthropogenically enhanced are not separated into anthropogenic and natural components. Purely anthropogenic emissions comprise over half of the atmospheric reservoir. Modified from *Selin* [2009].

Mercury in the atmosphere can be found in two different oxidation states, which interact with the environment in different ways. Elemental mercury (Hg^0), which is the form of mercury released naturally from the Earth and some anthropogenic sources, is not very reactive with other elements because of its insolubility; it is also the most abundant form of mercury in the atmosphere, with greater than 95% of mercury being comprised of Hg^0 [*Pleigel and Munthe,* 1995; *Lindberg and Stratton,* 1998; *Schroeder and Munthe,* 1998]. On the other hand, Hg^{2+} (also known as reactive gaseous mercury or RGM) is a much more reactive form of mercury; this species is necessary for the creation of methylmercury and its resultant toxic effects [*Ullrich et al.,* 2001]. Mercury also exists in the atmosphere in the form of particulate mercury, which has very slow deposition rates and is not extensively considered here. The oxidation states of mercury can change through reduction-oxidation reactions, which normally occur in the oceans and the atmosphere. In the atmosphere, the oxidation of Hg^0 to Hg^{2+} is thought to occur through a photochemical process [*Holmes et al.,* 2006]. However, the exact chemistry occurring in the atmosphere to oxidize mercury is not entirely understood [*Lin et al.,* 2006]. There are several oxidants that may be contributing to atmospheric mercury oxidation, including OH, O_3, and Br [*Seigneur and Lohman,* 2008; *Weiss-Penzias et al.,* 2009; *Holmes et al.,* 2006]. These reactions have different types of chemistry and reaction rates, which complicate the understanding of RGM levels in the atmosphere. Currently, bromine is considered

to be the primary mercury oxidant in the atmosphere [*Holmes et al.,* 2006; *Holmes et al.,* 2010].

Accurately understanding the processes occurring in the atmosphere is important for modeling global mercury transport. Global 3-D models of chemical transport, such as GEOS-Chem, can help researchers determine the processes by which mercury interacts with the environment, including transport and atmospheric chemistry, which could cause significant policy ramifications. However, in order for GEOS-Chem to be most useful in guiding decision-making, the model should accurately reproduce these chemical reactions and other transport processes. The accuracy of GEOS-Chem can be determined by comparing model results with actual observations. By examining discrepancies between the two, hypotheses can be made about which atmospheric processes are not accurately represented. These hypotheses can be tested using a simplified box model, where it is much easier to turn processes on and off to get a more accurate representation of the actual physics and chemistry occurring in the atmosphere that may affect mercury concentrations and diurnal trends.

The box model created in this study helps constrain some of the atmospheric processes thought to be occurring during the global biogeochemical mercury cycle over a terrestrial environment, which in turn will help make larger

scale atmospheric models, such as the GEOS-Chem model, more accurate. One previous attempt to quantify the chemistry and deposition of atmospheric mercury through the use of a box model was a paper by *Holmes et al.* [2009], which examined the sources and deposition of RGM in the marine environment. In that paper, a box model for mercury was created to interpret observations made over several marine sites. The box model from *Holmes et al.* [2009] described the mercury cycle over the oceans, including sources, sinks, chemical reactions, rates, and diurnal variations. This study compared observations over land sites (rather than marine sites, as has been done before) from *Weiss-Penzias et al.* [2009] with predicted measurements from the GEOS-Chem model. After comparing the GEOS-Chem results to measurements, a box model was created using techniques similar to *Holmes et al.* [2009] in order to gain a more accurate understanding of the physics and chemistry controlling mercury deposition over terrestrial environments on long-term and daily timescales. A better understanding of mercury deposition can improve model accuracy, which can help influence the path of policies related to mercury emissions in order to minimize mercury contamination and exposure.

The literature review section of this study will examine the health effects of mercury, oxidation, emissions, deposition, modeling techniques, and the modeling paper mentioned above. The methods section will discuss the *Weiss-*

Penzias et al. [2009] data, the GEOS-Chem model, and the methods used to compare the *Weiss-Penzias et al.* [2009] data and the GEOS-Chem model results. It will also discuss the creation of the box model and the parameters used within it. The analysis and discussion section will examine the differences between the Nevada data and the GEOS-Chem model results. It will also analyze the processes affecting the diurnal trend in the data. The conclusion section will address uncertainties and conclusions and will suggest future areas of research.

2. LITERATURE REVIEW

In order to address atmospheric mercury deposition and diurnal trends, several areas of mercury physics must be understood. First, this section will cover the health effects of mercury exposure to put mercury research into a broader context. Next, this review will cover the atmospheric chemistry of mercury, emissions (both anthropogenic and natural), mercury deposition, and modeling techniques. Finally, it will discuss an example of mercury deposition modeling using a one-box model.

2.1 Health Effects

Mercury is a dangerous toxin that is currently being regulated on national and international stages. Mercury's toxicity has been known for centuries. The phrase "mad as a hatter" is a reference to nineteenth century hat makers, who often worked in close quarters with mercury fumes, which caused severe neurological effects leading to a perceived insanity [*Buxton et al.,* 1965]. More recently, mercury's effects have been the target of much discussion in the policy community. Mercury is currently regulated by the U.S. Environmental Protection Agency (EPA) under the Clean Air Act (CAA) due to its toxicity and danger to human health [*Air Pollution Prevention and Control, U.S. Code*, 2008]. More recent proposed regulations included the 2005 Clean Air Mercury Rule (CAMR), which was part of the CAA and the first regulation to propose reductions of

mercury emissions from power plants [*Standards of Performance for New and Existing Stationary Sources: Electronic Utility Steam Generating Units, Code of Federal Regulations,* 2005]. However, CAMR was vacated by the D.C. Circuit Court in 2008 [*NJ v. EPA, D.C. Cir.,* 2008]. In response to the failure of CAMR, the EPA has updated the National Emission Standards for Hazardous Air Pollutants (NESHAP) as it applies to power plants to require that mercury be regulated using the maximum achievable control technology (MACT) [*NESHAP, Code of Federal Regulations,* 2011]. Mercury emissions are under debate on an international level through the United Nations Environment Programme Global Mercury Partnership (see http://hqweb.unep.org/hazardoussubstances/Mercury/GlobalMercuryPartnership/tabid/1253/language/en-US/Default.aspx).

Government attention to mercury stems from the effects of a molecule called methylmercury (CH_3Hg^+), which is the form of mercury of most concern to human health. Methylmercury is formed predominantly from the methylation of inorganic mercury in aqueous environments, which depends on temperature, pH, the presence of inorganic and organic agents, and the status of the sulfate-reducing bacteria that actually methylate mercury [*Ullrich et al.,* 2001; *Ravichandran*, 2004]. Methylmercury is so dangerous because when it binds with the cysteine amino acid the resultant structure highly resembles the methionine amino acid [*Kerper et al.,* 1992]. Methionine—and the methylmercury-cysteine

compound—easily pass the blood-brain barrier, thus allowing for direct delivery of methylmercury to the brain, where it accumulates and causes toxic effects [*Kerper et al.,* 1992; *Environmental Protection Agency (EPA),* 1997; *Mergler et al.,* 2007]. Methylmercury accumulates in the tissues of fish and other marine life, where it can be passed on to fish-eating populations, including humans [*Mergler et al.,* 2007]. Mercury poisoning can cause many neurological disorders, including cerebral palsy, deafness, ataxia, smaller brain size, and minor developmental delays, depending on exposure timescales and quantities [*Buxton et al.,* 1965; *World Health Organization (WHO),* 1990; *Castoldi et al.,* 2001]. Given the delicate nature of developing neural systems, exposure during childhood and *in utero* has greater negative effects than exposure later in life [*Mergler et al.,* 2007].

Given that methylmercury bioaccumulates (meaning that it becomes more and more concentrated up the food chain), humans are particularly at risk for mercury poisoning, as are other predatory species [*Mergler et al.,* 2007]. Human populations in the Arctic and those who rely on fish as a main source of nutrition are particularly at risk. However, methylmercury is found in fish that cross international and socio-economic boundaries, thus truly making mercury levels a global concern [*Mergler et al.,* 2007]. Considering the health benefits from a diet high in fish rich in omega-3 fatty acids, there is a tradeoff between healthy fats and mercury exposure [*Mergler et al.,* 2007].

The international aspect of mercury emissions, exposure, and transport makes mercury regulation a complicated issue. More research is being done to determine the lowest level mercury dose that would cause adverse effects. An understanding of how mercury interacts with the body and human development is a key part of establishing regulations and emission limits.

2.2 Atmospheric Chemistry

Elemental mercury (Hg^0) and reactive gaseous mercury (Hg^{2+})—also known as RGM—are the two most common species of mercury in the environment, but they behave quite differently. Mercury can also exist as Hg^+, but this oxidation state is not normally stable under environmental conditions [*Environmental Protection Agency (EPA),* 1997]. In addition to reactive gaseous mercury and elemental mercury, mercury in the atmosphere also exists in the particulate phase (HgP), which comprises some mercury of the Hg^{2+} oxidation state [*Selin et al.,* 2008]. Particulate mercury behaves similarly to reactive gaseous mercury in terms of deposition velocities and solubility [*Selin et al,* 2007; *Selin et al.,* 2008]. Hg^{2+} partitions between the particulate state and reactive gaseous mercury through a mechanism that is not well understood. As such, the analyses done here will ignore this partitioning, which introduces uncertainty.

The majority of mercury in the atmosphere is in the form of elemental mercury [*Pleigel and Munthe,* 1995; *Lindberg and Stratton,* 1998; *Schroeder and Munthe,* 1998]. Over terrestrial environments, elemental mercury may be as much as 83% of total gaseous mercury, while over marine environments it comprises about 90-95% of total gaseous mercury [*Slemr et al.,* 1985; *Pleigel and Munthe,* 1995]. The drop in elemental mercury percentage over land is due to the Hg^{2+} emissions coming from land sources rather than a drop in elemental mercury itself [*Slemr et al.,* 1985]; in areas of particularly heavy emissions, Hg^{2+} levels would be even higher [*Slemr et al.,* 1985]. Also, elemental mercury has a longer residence time in the atmosphere (on the order of months) compared to RGM and HgP (on the order of days to weeks) [*Selin et al.,* 2007; *Selin et al.,* 2008]. The longer residence time of elemental mercury allows it to travel far away from where it was emitted into the atmosphere before it is deposited.

Mercury passes between elemental and reactive gaseous mercury states in the atmosphere through reduction-oxidation reactions. Oxidation of Hg^0 to Hg^{2+} in the atmosphere occurs through photochemical processes, meaning that it is fueled by the sun, occurs during daylight hours, and occurs with various oxidants [*Jaffe et al.,* 2005]. There are several oxidants in the atmosphere that could be responsible for the oxidation of elemental mercury, some of which are displayed in Table 1.

Table 1. Mercury Oxidation Reactions, Oxidants, and Rate Constants. Rate constants are in cm^3 $molecule^{-1}$ s^{-1}. Taken from *Lin et al.*, [2006].

Mechanism	Oxidant	Rate Constant
$Hg^0+O_3 \rightarrow HgO+O_2$	O_3	$3\text{-}490 \times 10^{-20}$
$Hg^0+OH \rightarrow Hg^{2+}$ Products	OH	$8.7\text{-}9.0 \times 10^{-14}$
$Hg^0+Br_2 \rightarrow Hg^{2+}$ Products	Br_2	$<9 \times 10^{-17}$
$Hg^0+Br \rightarrow Hg^{2+}$ Products	Br	3.2×10^{-12}
$Hg^0+BrO \rightarrow Hg^{2+}$ Products	BrO	10^{-13}—10^{-15}

While many types of oxidation could be occurring, bromine reactions are more significant than others [*Holmes et al.*, 2006; *Holmes et al.*, 2010]. Previously, ozone and OH reactions were thought to be an important part in the oxidation process [*Hall*, 1995; *Selin et al.*, 2008]. However, the thermodynamics and kinetics of the atmosphere inhibit these reactions; they are not the most important oxidizers in the atmosphere and their reactions may not even be occurring [*Calvert et al.*, 2005]. More recent research has emphasized the importance of bromine because of its rate constant [*Wang and Pehkonen*, 2004; *Seigneur and Lohman*, 2008; *Holmes et al.*, 2006; *Holmes et al.*, 2010]. Reactive gaseous mercury concentrations fluctuate during the day, which can be explained

by the fluctuation in oxidant concentration due to the sun [*Lindberg and Stratton,* 1998; *Holmes et al.,* 2009; *Weiss-Penzias et al.,* 2009].One of the key steps of determining which oxidant is causing the production of RGM is to examine the time of day that the concentration of Hg^{2+} peaks; due to the difference between the diurnal oxidant concentrations for bromine and OH, the RGM peak occurs at different times of day; bromine chemistry causes a peak around noon, while OH chemistry causes a peak during the afternoon [*Holmes et al.,* 2009]. Given the current literature on mercury oxidation, bromine is considered the primary oxidant [*Holmes et al.,* 2009; *Holmes et al.,* 2010].

Another potentially important part of mercury atmospheric chemistry is the reduction of Hg^{2+} to Hg^{0}. However, the existence of mercury reduction reactions in the atmosphere is debated in the literature [*Lindberg et al.,* 2007]. Mercury reduction is significant in soils after Hg^{2+} has been deposited and also occurs in aqueous systems [*Lin et al.,* 2006; *Fritsche et al.,* 2008]. Overall, mercury reduction is much less understood than mercury oxidation.

Given the uncertainties in oxidation and reduction rates, understanding the chemistry well enough to model mercury deposition can be a challenge. In order to determine the amount of RGM produced from elemental mercury oxidation, the concentration of the oxidant in question must be known. However, many studies

use oxidant concentrations taken from model monthly means or back calculation to match results rather than measuring the oxidants themselves [*Park et al.,* 2004; *Holmes et al.,* 2009; *Weiss-Penzias et al.,* 2009].

2.2 Emissions

Mercury is used by and emitted from a variety of anthropogenic sources in multiple oxidation states across the world. Mercury serves an important role in industrial sectors where is can be used in chlorine production and as an additive to pharmaceutical products [*Environmental Protection Agency (EPA),* 1997]. It can also be used in fluorescent lamps, thermostats, batteries, barometers, and thermometers [*Environmental Protection Agency (EPA),* 1997]. In addition to more industrial uses, mercury played an important role in pre-industrial gold mining [*Strode et al.,* 2009]. Present anthropogenic emissions are about 3400 Mg per year, with about half of that coming from Asia [*Jaffe et al.,* 2005; *Pacyna et al.,* 2005]. However, given the lack of information about emission sources in developing countries, these numbers may be underestimated [*Jaffe et al.,* 2005; *Selin et al.,* 2008]. Anthropogenic sources are capable of emitting both Hg^0 and Hg^{2+}; most of the Hg^{2+} deposits nearby its source, while Hg^0 is capable of being transported much farther away due to its longer residence time [*Lin and Pehkonen,* 1999; *Gustin and Jaffe,* 2010]. Photochemical oxidation of Hg^0 can

lead to the deposition of Hg^{2+} farther away from anthropogenic sources, which complicates emission regulations [*Guentzel et al., 2001; Selin and Jacob,* 2008].

Mercury regulations are further complicated by natural emissions of mercury, which can occur from volcanic activity, soils, oceans, and naturally enriched mercury sites (see Figure 1, page 11) [*Selin,* 2009]. In some cases, mercury release is so high that it exceeds deposition [*Zhang et al.,* 2009]. Areas that are enriched in mercury include mercuriferous belts, which are located near plate tectonic boundaries and contain high levels of cinnabar ore (HgS) [*Varekamp and Buseck,* 1986]. Nevada, which is the focus of this study, is a naturally enriched region [*Coolbaugh et al.,* 2002]. Volcanoes also release large amounts of mercury, which can have more global effects if the eruption extends high enough in the atmosphere to enter the global circulation [*Varekamp and Buseck,* 1986]. Most mercury released naturally is in the form of Hg^0 [*Gustin et al.,* 2003].

Elemental mercury is also released from soils and the ocean after it is deposited and is emitted through biomass burning [*Selin et al.,* 2008]. This type of emission occurs relatively rapidly after the mercury is deposited. Biomass burning, which is anthropogenically enhanced, releases stored mercury to the atmosphere [*Weiss-Penzias et al.,* 2007]. Some elemental mercury emissions are

[*Fritsche et al.,* 2008]. In some studies, the mercury release from soils follows a diurnal pattern based on solar radiation, soil temperature, and soil moisture and therefore peaks during daylight hours [*Carpi and Lindberg,* 1998].

Although these mercury emissions occur as the result of natural processes, the flux of mercury coming from many natural sources has been enhanced by anthropogenic activities [*Selin,* 2009]. Figure 1 (page 11) shows the relative magnitudes of different emission processes. By assessing mercury levels in sediment records from lakes, modern and preindustrial deposition rates can be determined, which confirm that anthropogenic mercury emissions (which peaked during the middle of the twentieth century) are have increased deposition by a factor of three to five [*Swain et al.,* 1992; *Pirrone et al.,* 1998; *Perry et al.,* 2005]

2.3 Deposition

Mercury reaches the land and ocean surfaces through deposition, but the multiple types of mercury deposit at different rates and through different mechanisms. There are two types of deposition: dry deposition and wet deposition. Wet deposition occurs during rainfall events, while dry deposition is a settling process that occurs without precipitation and is influenced by atmospheric turbulence and chemical properties [*Seinfeld and Pandis,* 1998]. Elemental mercury is less soluble than other forms of mercury because of its low Henry's

law constant and is therefore less susceptible to wet deposition than the more soluble Hg^{2+} and HgP [*Lin and Pehkonen,* 1999; *Mason and Sheu,* 2002]. In fact, most mercury deposition—both dry and wet—is of mercury in Hg^{2+} and HgP states [*Landis et al.,* 2002]. Elemental mercury has an atmospheric residence time of about one year, while Hg^{2+} and HgP have much shorter residence times on the order of days to weeks [*Pehkonon and Lin,* 1998; *Mason and Sheu,* 2002; *Selin et al.,* 2007; *Selin et al.,* 2008]. As such, elemental mercury is capable of traveling much farther distances in the atmosphere before it deposits than the other forms of mercury, which are more likely to deposit nearby their production locales. However, since elemental mercury oxidizes to form RGM and particulate mercury, these forms of mercury can be present far away from any apparent sources [*Engle et al.,* 2010].

Different species of mercury undergo dry deposition at different velocities due to various factors; deposition rates can be determined through modeling and direct measurements [*Holmes et al.,* 2009; *Zhang et al.,* 2009]. Deposition velocities also vary depending on location, time of day, and time of year and have been modeled as a function of aerodynamic resistance, quasi-laminar layer resistance, and canopy resistance [*Seinfeld and Pandis,* 1998; *Zhang et al.,* 2009]. Dry deposition velocities of Hg^0 are between 0.1-0.4 cm s^{-1} over vegetated areas, but are much smaller over non-vegetated areas [*Zhang et al.,* 2009]. RGM

deposits much faster, between 0.5-6 cm s^{-1}, while HgP deposits at a rate of 0.02-2 cm s^{-1} [*Zhang et al.,* 2009]. These deposition velocities are from observed measurements, but there are methods to estimate dry deposition velocities using transport models and considering atmospheric processes such as wind speed and friction velocity [*Stull,* 1988; *Seinfeld and Pandis,* 1998]. For example, calculations by *Holmes et al.* [2009] of the RGM dry deposition velocity put the figure closer to 0.4-1.4 cm s^{-1}, which is a much narrower range of values and is in the smaller range of deposition velocities compared to the values collected by *Zhang et al.,* [2009]. One of the key issues that affects dry deposition velocities is the exact nature of the air-surface interface; differences in re-emission rates of Hg^0 can affect dry deposition rates [*Zhang et al.,* 2009]. The relative deposition velocities of the three mercury species are consistent with the relative residence times of mercury species; longer-lived elemental mercury has a slower deposition velocity, while shorter-lived RGM has a faster deposition velocity [*Zhang et al.,* 2009]. Given the wide range of deposition velocities found in current literature, choosing a concrete value for modeling exercises can be rather difficult, especially considering all the factors that can affect dry deposition.

2.5 Modeling

Modeling mercury deposition, transport, and chemistry can be done with many different types of models, ranging from simple one-box models to more

complicated global 3-D chemical transport models. One of the most common models used in advanced mercury research is the GEOS-Chem model, which is a global 3-D chemical transport model driven by assimilated meteorological observations from the Goddard Earth Observing System (GEOS) of the NASA Data Assimilation Office (DAO) [*Bey et al.,* 2001]. The model includes many different processes, including weather events, chemistry, emissions, and deposition [*Bey et al.,* 2001]. It can be run using a wide range of parameters to track specific elements, one of which is mercury [*Bey et al.,* 2001]. Also, it can predict these processes for particular past time ranges using known weather and climate information. The GEOS-Chem model has been used to examine a wide range of atmospheric processes and is commonly used to model mercury, both in terms of purely atmospheric processes and atmospheric-oceanic interactions [see *Selin et al.,* 2007; *Strode et al.,* 2007; *Selin et al.,* 2008; *Holmes et al.,* 2010; *Soerensen et al.,* 2010].

2.6 Box Model Example

Box models have been used to analyze the sources and deposition of mercury before, such as in *Holmes et al.,* [2009], which analyzed elemental and reactive gaseous mercury in the marine atmosphere using a box model and data taken during cruises of the remote Atlantic, the remote Pacific, and coastal Japan [see *Laurier et al.,* 2003; *Jaffe et al.,* 2005; *Laurier and Mason,* 2007]. The paper

by *Holmes et al.* [2009] developed a box model of the marine boundary layer described by the equation

$$\frac{dc}{dt} = P - L + \frac{F_e - F_d}{Z} - J, \quad (1)$$

where P represents chemical production, L represents chemical loss, F_e represents entrainment flux from the free troposphere, F_d represents deposition flux to the surface, Z represents the boundary layer height, and J represents uptake by sea-salt aerosols. Integrating this equation using the MATLAB ode15s algorithm yielded a diurnal variability in reactive gaseous mercury—which was also observed in the cruise data—and hypothesized that this trend was due to photochemical bromine oxidation and RGM uptake into sea-salt aerosols [*Holmes et al.,* 2009]. This paper did not see any significant diurnal variation in elemental mercury, leading to the conclusion that the reaction rate of bromine oxidation is slower than originally assumed [see *Holmes et al.,* 2009, and references therein].

3. METHODS

This section will cover the methods used in this paper, starting with a description of the GEOS-Chem model parameters and the *Weiss-Penzias et al.* [2009] Nevada measurements that the GEOS-Chem data were compared against. Next, this section will review the methods used to compare data from the GEOS-Chem model runs and the Nevada measurements. Finally, this section will review the methods behind creating a box model for mercury deposition over land.

3.1 GEOS-Chem Model

The global 3-D GEOS-Chem chemical transport model was run using many parameters to analyze the transport, chemistry, and deposition of elemental and reactive gaseous mercury [*Selin et al.*, 2007; *Selin et al.*, 2008]. In addition to representing atmospheric processes, GEOS-Chem also represents atmospheric-oceanic coupling of mercury, which includes deposition and photochemical and biological cycling between elemental and gaseous mercury in the mixed layer of the ocean [*Strode et al.*, 2007; *Selin et al.*, 2008]. The GEOS-Chem model uses assimilated meteorological data from the NASA Goddard Earth Observing System (GEOS-4) [*Bey et al.*, 2001]. This data includes temperatures, winds, precipitation, mixed layer depths, and convective mass fluxes, which are all taken every six hours with a horizontal resolution of $1° \times 1.25°$ and 55 hybrid sigma-pressure levels in the vertical [*Selin et al.*, 2007; *Selin et al.*, 2008]. However, the

GEOS-4 data is reduced in resolution for GEOS-Chem down to a horizontal resolution of 2° × 2.5° [*Bey et al.,* 2001; *Selin et al.,* 2007; *Selin et al.,* 2008].

GEOS-Chem can be run using multiple types of mercury oxidation chemistries,,including OH, O_3, and Br and includes other processes as well [*Selin et al.,* 2008; *Holmes et al.,* 2010]. The model includes Hg^{2+} partitioning between reactive gaseous mercury and particulate phases; however, the mechanism behind this partitioning is not well understood [*Selin et al.,* 2008]. For this reason, particulate mercury was ignored in this study and all Hg^{2+} was taken to be reactive gaseous mercury. GEOS-Chem also includes mercury emissions according to their actual magnitude and location in Nevada, as well as a re-emission source [*Selin et al.,* 2008]. All mercury emissions in the GEOS-Chem model are taken to be of elemental mercury [*Selin et al.,* 2008]. Other components of the GEOS-Chem model include prompt mercury recycling, evapotranspiration, biomass burning, and soil volatilization [*Selin et al.,* 2008].

For this study, GEOS-Chem was run for June, July, and August of 2007. Hourly concentrations of Hg^0, Hg^{2+}, and HgP were determined from this three month model run for three sites in the Mercury Deposition Network, which included NV02, NV98, and DRI, and can be seen in Figure 2.

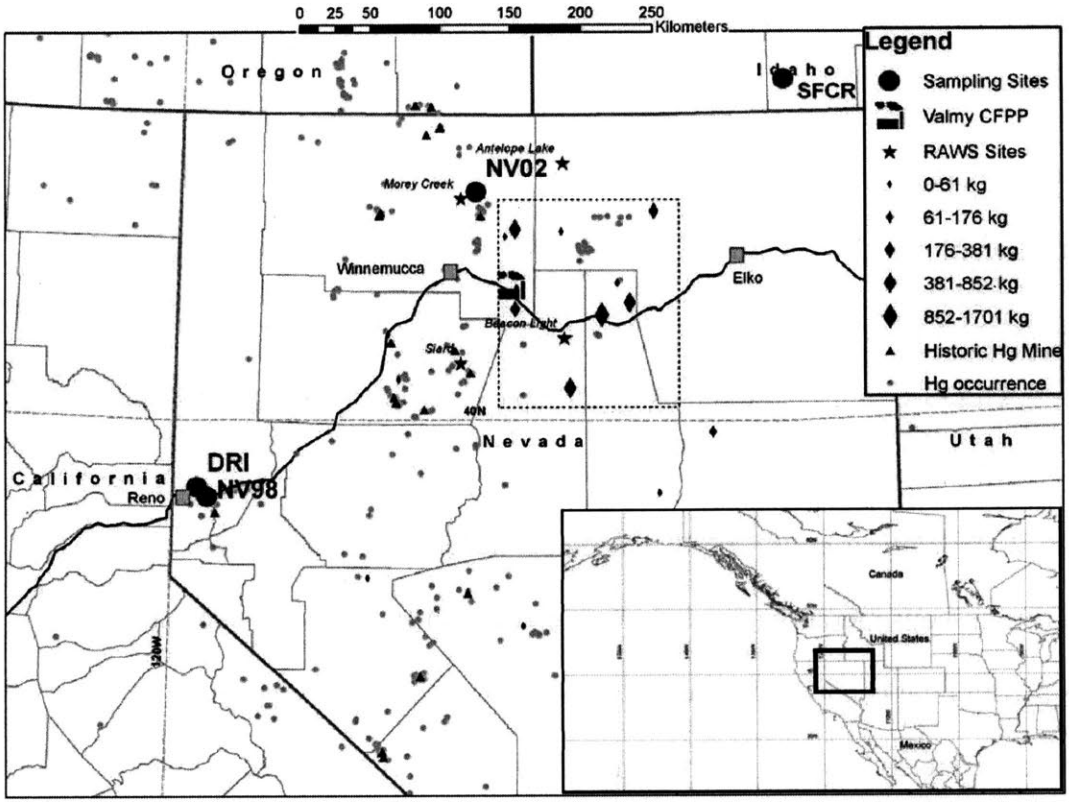

Figure 2. Map of the Nevada Sampling Sites. Note the locations of DRI, NV98, and NV02. Also note the location of known geologic deposits and anthropogenic emissions. From *Weiss-Penzias et al.* [2009].

In addition to running the GEOS-Chem model with bromine chemistry, the model was run using OH/O_3 chemistry. All of the mercury-oxidant chemistries can be found in Table 2. Note that all of the equations for a particular oxidant are part of the oxidation process and have individual rate constants.

Table 2. Elemental Mercury Oxidation Reactions. This table shows the elemental mercury oxidation reactions. Note that all of the equations for a particular oxidant are part of the oxidation process and have individual rate constants. Reactions taken from *Pal and Ariya* [2004a], *Pal and Ariya* [2004b], and *Holmes et al.* [2006].

OH Chemistry	O_3 Chemistry	Br Chemistry
$Hg^0 + OH \rightarrow HgOH$	$Hg_0 + O_3 \rightarrow HgO + O_2$	$Hg + Br \rightarrow HgBr$
$HgOH + OH \rightarrow Hg(OH)_2$		$HgBr \rightarrow Hg + Br$
$HgOH + HgOH \rightarrow Hg_2(OH)_2$		$HgBr + X \rightarrow HgBrX$ (X= Br, OH)

3.2 Nevada Measurements

In a paper by *Weiss-Penzias et al.,* [2009], researchers examined elemental, particulate, and reactive gaseous mercury deposition over three sites in Nevada. These sites are part of the Mercury Deposition Network (MDN) and are called NV02, NV98 and DRI (see Figure 2 for sites locations). All three sites have different local sources of mercury, including industrial activity and active gold mines (see Figure 2 for emissions locations). NV02 is located near a desert valley and is near two anthropogenic mercury sources [*Weiss-Penzias, et al.,* 2009]. NV98 is located near Reno, Nevada and is not near any major anthropogenic mercury sources; it is near areas of natural mercury enrichment [*Weiss-Penzias et al.,* 2009]. DRI is located near Reno, Nevada as well and is at a much higher altitude than the other sites. DRI is near a mining area that has known gold and mercury deposits [*Weiss-Penzias et al.,* 2009]. Given the sites' lack of proximity

to major anthropogenic and natural mercury sources, the reactive gaseous mercury measurements are higher than expected, meaning that Hg^0 oxidation must be creating Hg^{2+} in the atmosphere in addition to enhanced RGM deposition from the free troposphere [*Weiss-Penzias et al.,* 2009]. This paper observed a diurnal variation in RGM meaning that photochemical oxidation was a key factor in the mercury budget for the area, which *Weiss-Penzias et al.* [2009] attributed to ozone and OH.

3.3 Comparison of GEOS-Chem and Nevada Measurements

Model runs of the GEOS-Chem model and measurements from *Weiss-Penzias et al.* [2009] were compared to determine how well the GEOS-Chem is capable of modeling mercury transport and deposition over land. These datasets were compared on two different time scales. First, the measurements were compared over a one-month period of sampling (July 2007). This was done by plotting the mercury concentrations for both the GEOS-Chem and the Nevada measurements as a function of measurement time and date. This was done for both bromine and OH chemistry GEOS-Chem model runs even though current research emphasizes that most oxidation is occurring due to bromine [*Holmes et al.,* 2010]. Also, since the *Weiss-Penzias et al.* [2009] measurements were taken at three sites (NV02, NV98, and DRI), these comparisons were made at all three

sites. It is important to note that NV98 and DRI are located in the same grid-box in the GEOS-Chem model, so their model runs are identical.

Next, the data were examined to look at daily patterns and variations. For all data sets, a moving daily average was taken. The daily averages were subtracted from their corresponding hourly measurements, which yielded a set of data points that showed the hourly deviation from the daily mean for each day. Finally, the hourly variations were averaged to yield one value for the deviation from the daily mean for each hour. For example, all of the 1:00 variations from the respective daily means were themselves averaged to yield a mean 1:00 deviation. This was done for all hours to determine the entire daily profile for Hg^{2+}. By taking a daily average for every day, the effects of precipitation and weather were removed from the data. After examining differences between the GEOS-Chem model runs and the *Weiss-Penzias et al.* [2009] data, hypotheses were made concerning the reasons why the results were different, which will be reviewed in the analysis and discussion section.

3.4 Box Model

In order to test the hypotheses made from the GEOS-Chem and *Weiss-Penzias et al.* [2009] comparisons, a box model was created. A box model is one of the most simple model types, especially compared to complex models like

GEOS-Chem. Box models aid in determining the concentration of an element/oxidation species within a specified "box," which is normally the atmospheric boundary layer. Box models split up the processes occurring in the atmosphere into two main categories: processes adding to the concentration of the element in question and processes subtracting from the concentration of the element in question. These processes normally include events such as emissions, deposition, chemistry, and transport. This box model was created in order to easily change the parameters identified from the comparison of the GEOS-Chem model and the *Weiss-Penzias et al.* [2009] measurements.

The box model in this study has several main components: transport, deposition, emissions, chemical loss, chemical production, and entrainment (see Figure 3, page 38) [*Jacob,* 1999]. These components all act at different rates and are controlled differently. For this study, it was important to consider elemental mercury and reactive gaseous mercury separately, although their concentrations are linked.

For the box model, some variables are taken to be constrained, while others are taken to be free. Given that diurnal variations were of interest in this study, parameters that fluctuate on a daily basis were taken to be free, which include Hg^0 emissions, oxidation, and the RGM concentration the free

troposphere. Also, since RGM deposition velocities in the literature have a wide range, reactive gaseous mercury dry deposition acts as somewhat of a free parameter as well within its described bounds. The completely constrained parameters include the entrainment velocity, the boundary layer height, and the dry deposition velocity for elemental mercury.

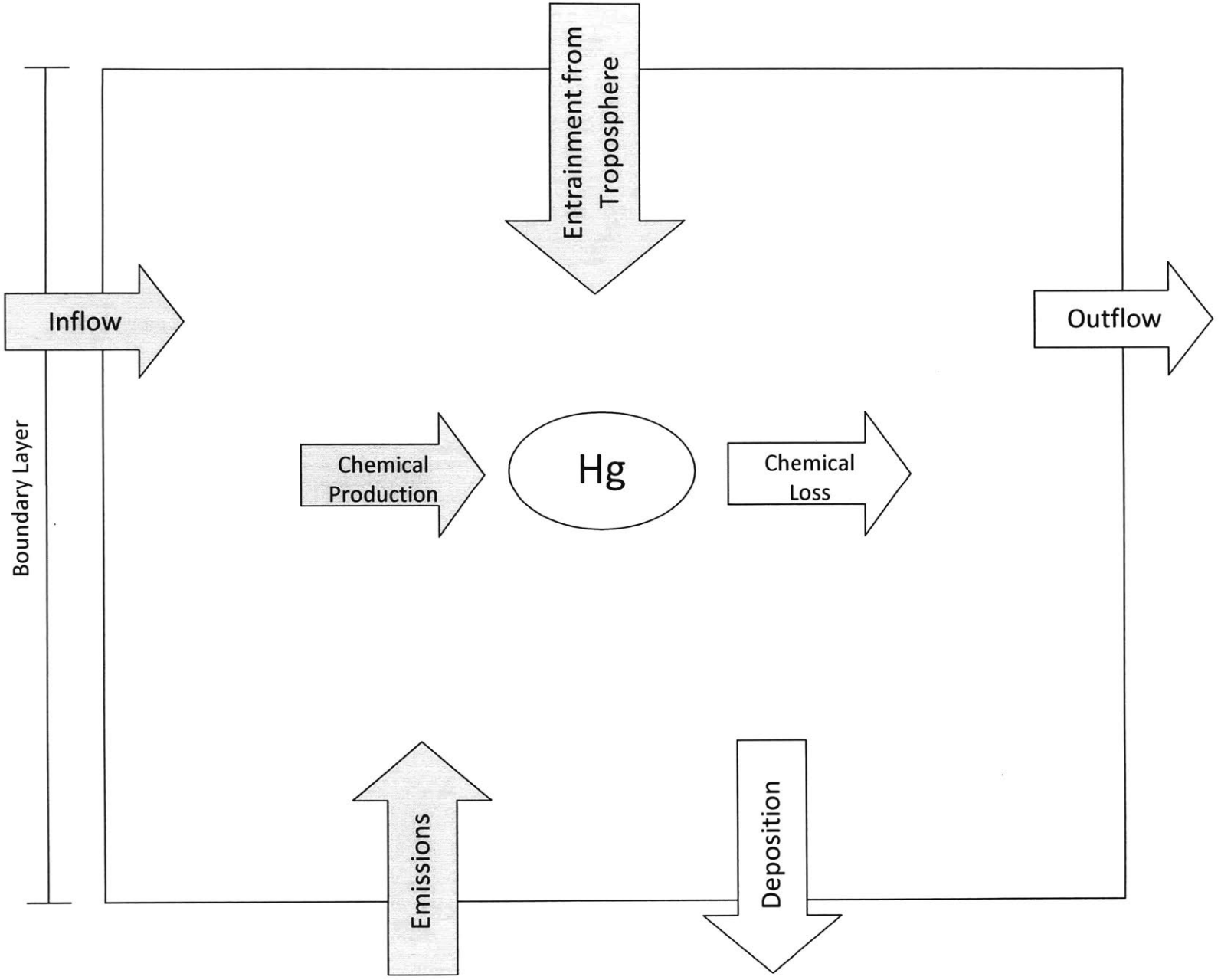

Figure 3. Box Model Diagram. This figure depicts the processes occurring in a one-box model of atmospheric mercury. Shaded arrows indicate processes that add to the concentration of mercury, and un-shaded arrows indicate processes that subtract from the concentration of mercury. Note that the species of mercury is not specified in this diagram, making it applicable to multiple species. Between species, the rates and concentrations of various parameters will change. Modified from *Jacob* [1999].

3.4.1 Transport

In the case of this study, it is assumed that transport in and out of the box are equal for both mercury species, meaning that the concentration of mercury in air entering the box is equal to the concentration of air leaving the box. This is accurate when the box is assumed to be the global atmosphere rather than a very small regional box [*Jacob,* 1999]. Also, since this study is mainly concerned with diurnal variations in mercury, transport can be neglected if it doesn't change systematically and consistently during course of the day. Transport was also neglected in the box model study by *Holmes et al.* [2009]. Transport is a constrained value due to the assumptions mentioned earlier.

3.4.2 Deposition

Deposition is an important process for both mercury species. This model considers dry deposition for elemental and reactive gaseous mercury. As mentioned earlier, elemental mercury has a relatively slow dry deposition velocity. For this study, a deposition velocity, v_{de}, of 3.6 m hr^{-1} was used, which equates to 0.1 cm s^{-1}. This is in the lower range of the target specified by *Zhang et al.* [2009] due to the desert location. Reactive gaseous mercury has a much faster dry deposition velocity [*Lindberg and Stratton,* 1998; *Zhang et al.,* 2009]. For this study, a deposition velocity, v_{dr}, of 36 m hr^{-1} was used, which equates to 1 cm s^{-1}, which is on the lower end of the range set by *Zhang et al.* [2009] partially to

account for the deposition over a desert environment. Considering the extensive literature on the subject of deposition and the known environment over which deposition is occurring, deposition was taken to be a somewhat free parameter within the range given by *Zhang et al.* [2009].

3.4.3 Emissions

Emissions from the land surface occur through several processes, including biomass burning, soil emissions, rapid recycling, volcanic emissions, and anthropogenic emissions (see Figure 1, page 11) [*Selin,* 2009]. Given the local of the Nevada sources, emissions would be coming from the soil, rapid recycling, and anthropogenic sources, with the anthropogenic sources including both industrial activity and active gold mining [*Lyman and Gustin,* 2007; *Weiss-Penzias et al.,* 2009]. Including volcanic emissions, oceanic emissions, and biomass burning in this box model would not make sense because of the site locations. The land near the Nevada sites has anthropogenic sources both in terms of industrial activity and active gold mining [*Weiss-Penzias et al.,* 2009].

Estimating the magnitude of sources for a box model can be difficult, especially because the estimates for emissions are given in global yearly averages that many not be accurate when scaled down to such small areas and timescales. However, there have been many local emissions studies of the Southwest United

States, including *Coolbaugh et al.* [2002], *Gustin et al.* [2003], and *Lyman and Gustin* [2008]. Most natural emissions are in the form of elemental mercury and would therefore be present in the Hg^0 box model equation [*Selin et al.,* 2008]. Natural sources of elemental mercury would emit about 28 pg/m^3 hr due to the mercury enrichment near mining districts, the desert landscape, and boundary layer height [*Coolbaugh et al.,* 2002; *Gustin et al.,* 2003]. Natural emissions would follow a diurnal trend because Hg^0 emissions vary depending on solar radiation, soil temperature, and soil moisture [*Carpi and Lindberg,* 1998]. This diurnal trend is parameterized in the box model by assuming that emissions are zero at night, start rising at 6:00, peak at midday, and then decrease in the afternoon until 18:00 after which they are zero again.

Anthropogenic emissions are often taken to be completely comprised of elemental mercury, although this can vary in other studies by as much as 50% [*Swain et al.,* 1992; *Gustin,* 2003; *Lyman and Gustin,* 2008; *Selin et al.,* 2008]. Anthropogenic emissions would add to the Hg^0 total, but not much considering the sites' lack of proximity to large industrial enterprises. As such, the total Hg^0 emissions, E_e, would be about 30 pg/m^3 hr, assuming a 2 pg/m^3 hr anthropogenic emission. Given the lack of knowledge of small scale elemental mercury emissions, including the influence of the sun, Hg^0 emissions are a free parameter.

Given the small level of anthropogenic emissions occurring near the Nevada sites due to gold mining and some smaller-sized anthropogenic sources, there would be a small amount of Hg^{2+} emissions, but in some studies, including this one, it has been assumed that all emissions would be completely comprised of elemental mercury [*Selin et al.,* 2008; *Weiss-Penzias et al.,* 2009].

3.4.4 Chemical Loss/Production

As mentioned in the background section, the rate of the oxidation reaction is under much debate because the physics occurring in the atmosphere is not completely understood. In the atmosphere, only oxidation from Hg^0 to Hg^{2+} is occurring, which means that in this box model chemical loss is occurring for Hg^0 while chemical production is occurring for Hg^{2+} [*Selin et al.,* 2007]. Generally, the ability of ozone and OH to be the main oxidant in question is becoming less supported by science while bromine oxidation is becoming a much more likely candidate [*Wang and Pehkonen,* 2004; *Calvert and Lindberg,* 2005; *Seigneur and Lohman,* 2008; *Holmes et al.,* 2010]. As such, there is a wide range of rate constants that could be used, as seen in Table 1. Oxidation reactions are shown in Table 2. Ozone was not considered in the box model analysis.

In addition to there being a wide range of rate constants, this box model requires the concentration of the oxidant itself, which varies over the course of the

day. Given that this quantity is not often measured in conjunction with mercury levels, there could be very diverse possible values that could drastically affect the chemistry occurring in the box model. Bromine and OH peak at different times of day due to their photochemical properties. The daily oxidant profiles are shown in Figure 4. For this box model, the concentration of the oxidant was multiplied by a diurnal trend, which is shown in Figure 4 for both Br and OH. The diurnal trend was reduced to a maximum of one rather than the higher concentrations shown Figure 4 in order to produce a signal where the maximum oxidant concentration is the same as its measured quantity rather than scaled up unrealistically.

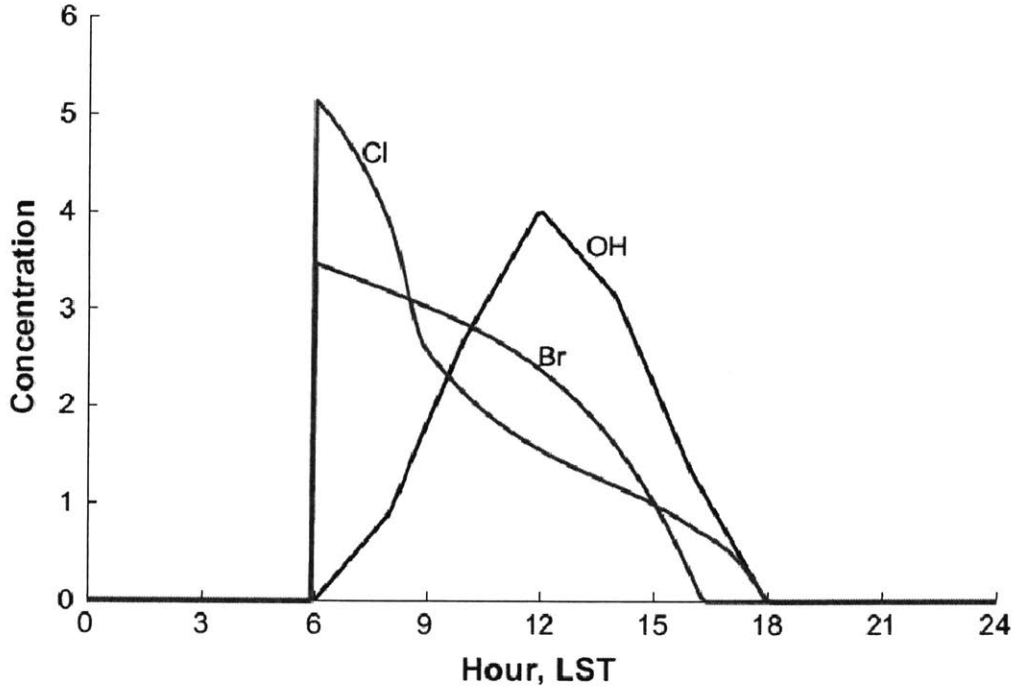

Figure 4. Diurnal Profiles of Oxidants. Note that only Br and OH were used in this study. Taken from *Holmes et al.* [2009]. See references therein.

Considering the broad uncertainties about which oxidants are important and the rates at which they act, chemical production and loss are most certainly a free parameter for this model, with the concentration of the oxidant in the box model being allowed to fluctuate between model runs to more accurately depict the chemistry occurring in the atmosphere and the observed diurnal amplitude. This study used a bromine concentration, *[oxidant]*, of 5×10^{11} molec./m^3, which is on the low side of the range described by *Seigneur and Lohman* [2008]. A second order rate constant, *k*, of 5.5×10^{-15} m^3/molecule hr was used, which was an overall rate constant for the entire Hg^0 oxidation reaction that was found by averaging overall rate constants from five different studies [see *Seigneur and Lohman,* 2008 and references therein]. For completeness sake, a box model for OH oxidation was also made in order to confirm its inappropriateness for mercury oxidation. An overall rate constant, *k,* of 2.56×10^{-16} m^3/molecule hr was used, which was consistent with *Hall et al.* [1995]. The concentration of OH was taken to be 1×10^{12} molec./m^3 [*Holmes et al.*, 2010].

3.4.5 Entrainment

Entrainment is a process by which air from the upper troposphere subsides into the boundary layer. Over land, boundary layer heights can be on the order of 1 km, but are smaller over deserts [*He et al.*, 2010]. In this case, the boundary

layer was taken to be 750 m, which is consistent with *Holmes et al.* [2009]. In the upper atmosphere, the concentration of Hg^{2+} is higher than it is in boundary layer because there is a lack of removal through dry deposition [*Lindberg et al.,* 2007]. On the other hand, the concentration of Hg^0 is lower than that of the boundary layer [*Lindberg et al.,* 2007]. The background concentration of Hg^{2+} in the free troposphere, c_{ftr}, is 43 pg/m^3 [*Swartzendruber et al.,* 2006] . The concentration of Hg^0 in the free troposphere, c_{fte}, is 1540 pg/m^3 [*Swartzendruber et al.,* 2006]. The entrainment velocity, v_e, used was 18 m/hr, which was the same as the entrainment velocity used by *Holmes et al.* [2009].

As vertical mixing changes during the day and oxidation occurs in the free troposphere, the amount of mercury fluxing down into the boundary layer changes, which causes a diurnal signal in boundary layer where reactive gaseous mercury peaks during the day [*Swartzendruber et al.,* 2006; *Selin et al.,* 2007; *Faïn et al.,* 2009; *Weiss-Penzias et al.,* 2009]. The average daily peak was taken to be 66 pg/m^3 and is represented in the box model through a time dependent entrainment that peaks at midday [*Swartzendruber et al.,* 2006]. In previous studies, the flux of reactive gaseous mercury entrainment from the free troposphere was taken to completely explain the RGM diurnal signal. RGM entrainment from the free troposphere was taken to be a free parameter in that the free troposphere Hg^{2+} concentration would be allowed to increase to 600 pg/m^3

between model runs, which was the maximum enhancement seen in *Swartzendruber et al.* [2006].

3.4.6 Box Model Equation

The overall equations for the box model are

$$\text{Hg}^0: \qquad \frac{dc_e}{dt} = -kc_e[oxidant] + E_e + \frac{v_e}{z}(c_{fte} - c_e) - \frac{v_{de}}{z}c_e, \tag{2}$$

$$\text{Hg}^{2+}: \qquad \frac{dc_r}{dt} = kc_e[oxidant] + \frac{v_e}{z}(c_{ftr} - c_r) - \frac{v_{dr}}{z}c_r, \tag{3}$$

where c_e and c_r are the concentrations of elemental and reactive gaseous mercury, respectively, in pg/m^3. All of the rates are per hour. A summary of parameters can be seen in Table 3.

Table 3. Initial Parameters Used in the Box Model. These are the parameters that were used in the box model described in the Methods section. Note that the terminology is consistent with the model and that sources are listed. Also note that units are in terms of centimeters rather than the meters used in the box model and the text. Rates are per the hour.

Parameter	Value	Source
v_{de}	360 cm/hr	*Zhang et al.* [2009]
v_{dr}	3600 cm/hr	*Zhang et al.* [2009]
E_e	3×10^{-5} pg/cm^3 hr	*Coolbaugh et al.* [2002]
v_e	1800 cm/hr	*Swartzendruber et al.* [2006]
c_{fte}	1.54×10^{-3} pg/cm^3	*Swartzendruber et al.* [2006]
c_{ftr}	4.3×10^{-5} pg/m^3	*Swartzendruber et al.* [2006]
k, Br	5.5×10^{-9} cm^3/molec. hr	*Seigneur and Lohman* [2008]
[Br]	5×10^{5} molec./cm^3	*Seigneur and Lohman* [2008]
k, OH	2.56×10^{-10} cm^3/molec. hr	*Swartzendruber et al.* [2006]
[OH]	1×10^{6} molec./cm^3	*Seigneur and Lohman* [2008]

Time specific processes include the oxidation of Hg^0 (according to the concentration of oxidant as seem in Figure 4), elemental mercury emissions, and entrainment from the free troposphere. The equations were programmed into MATLAB and solved using ode15s for ten days before the last day was analyzed.

4. ANALYSIS AND DISCUSSION

This section will review discrepancies between the GEOS-Chem model and the *Weiss-Penzias et al.* [2009] data, including elemental mercury means and reactive gaseous mercury diurnal amplitudes. This section will also use the box model to conduct sensitivity simulations to assess the influence of different parameters on the diurnal cycle of RGM.

4.1 Elemental Mercury Means

This section consists of graphs of the long-term comparisons between GEOS-Chem model runs and the *Weiss-Penzias et al.* [2009] measurements from Nevada during July of 2007. Graphs shown here are the long-term comparisons for all three sites (NV02, DRI, and NV98). Comparisons are shown for the Br chemistry, while OH chemistry graphs can be found in Appendix 2.

As shown in Figures 5-7, GEOS-Chem is under-predicting the day-to-day diurnal amplitude of elemental mercury concentration as well as the mean elemental mercury concentration. Figure 5 shows the long-term comparison for NV02. It is an hourly plot of Hg^0 concentrations for GEOS-Chem and the *Weiss-Penzias et al.* [2009] data during July 2007. Figure 6 is the same plot for NV98 and also shows the same under-prediction trend in both quantities. Figure 7 is the same plot for DRI. It also shows an under-prediction of the diurnal amplitude of

Hg^0, but shows an over-prediction of the mean concentration of Hg^0, which is different than the other two sites.

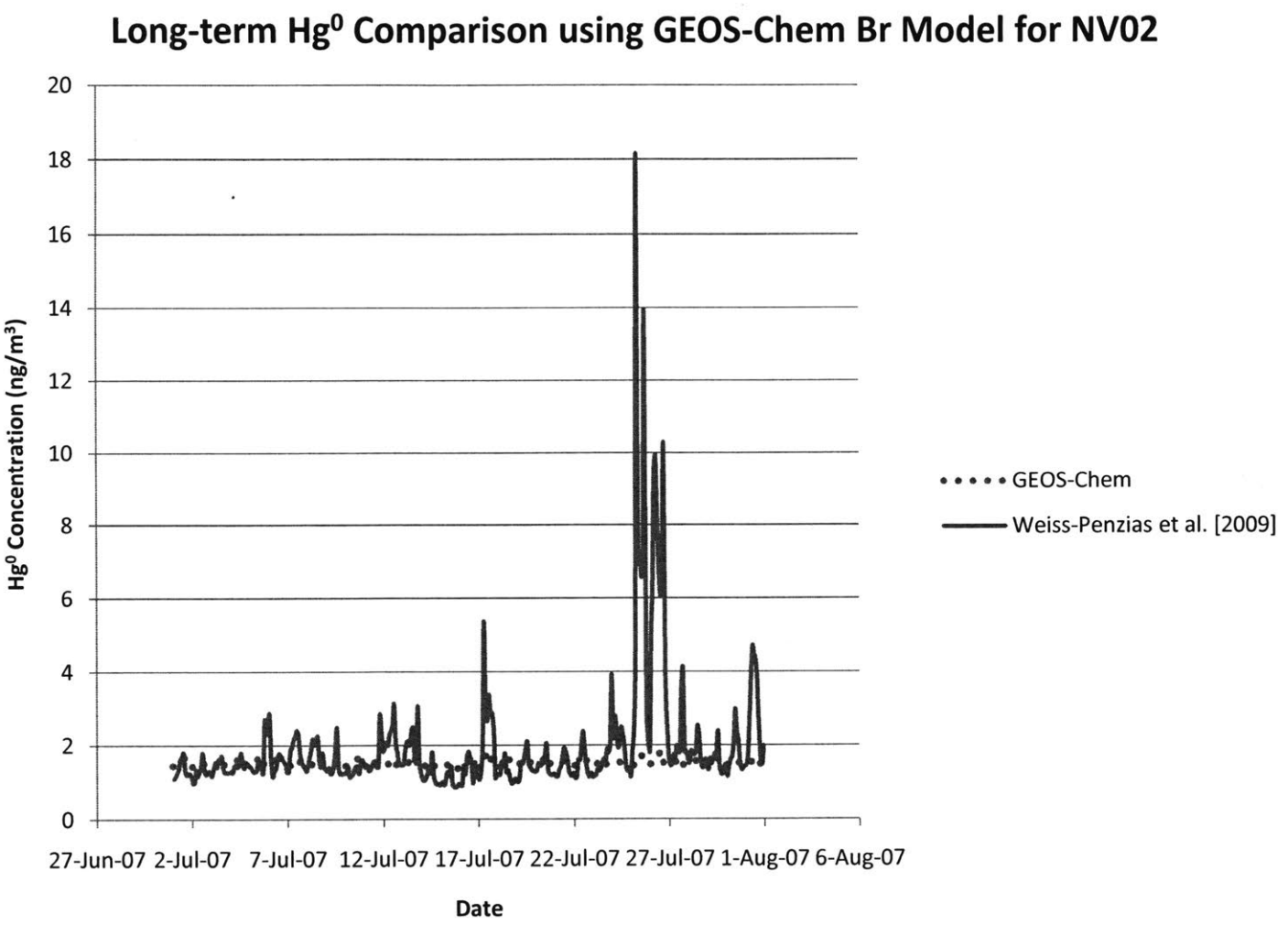

Figure 5. Long-term Hg^0 Comparison using GEOS-Chem Br Model for NV02. The solid line represents data from *Weiss-Penzias et al.* [2009] and the dashed line represents the GEOS-Chem model run data using Br chemistry. Note that the *Weiss-Penzias et al.* [2009] data has a higher amplitude of variation and tends to have a higher absolute value.

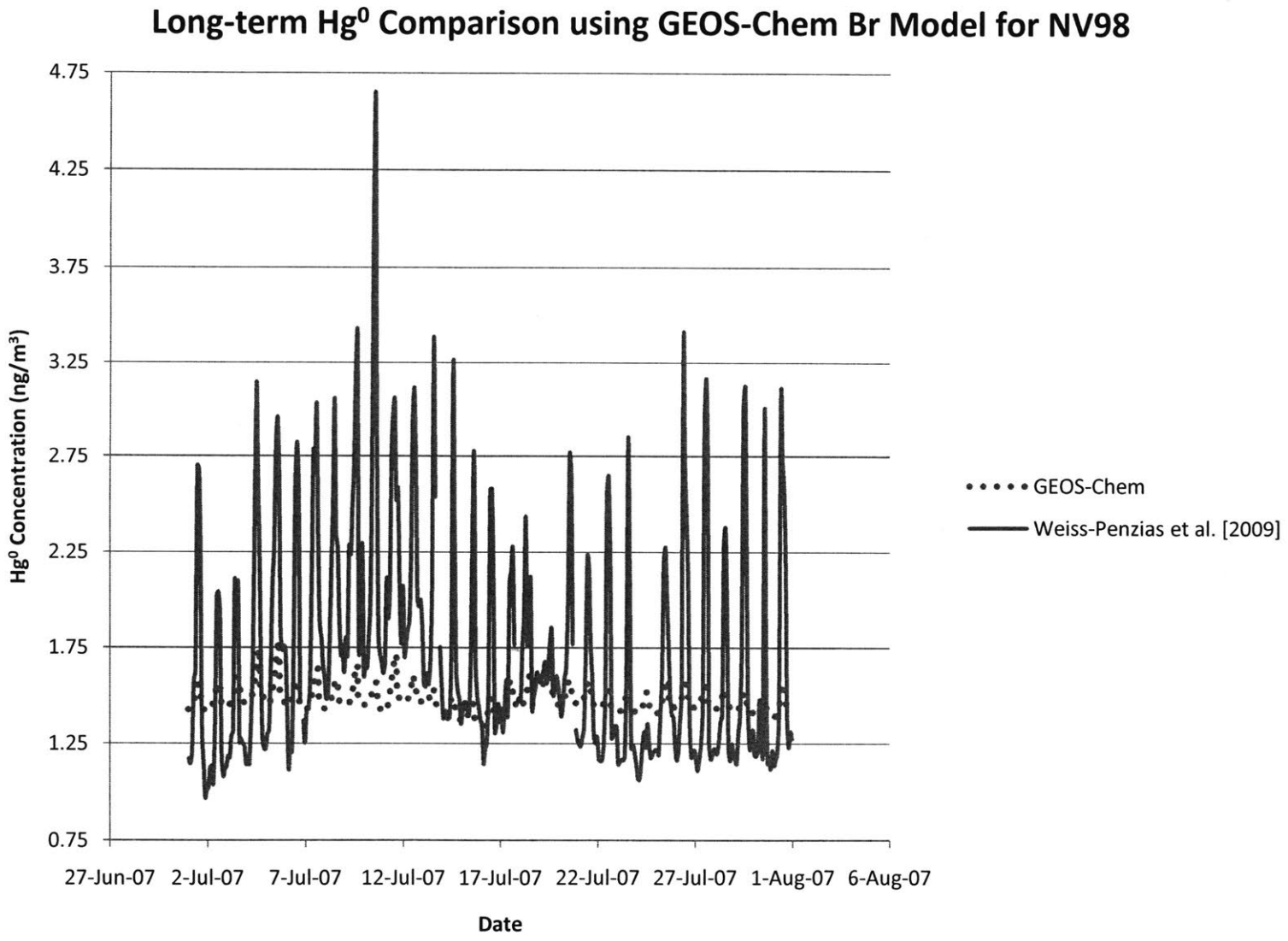

Figure 6. Long-term Hg^0 Comparison using GEOS-Chem Br Model for NV98. The solid line represents data from *Weiss-Penzias et al.* [2009] and the dashed line represents the GEOS-Chem model run data using Br chemistry. Note that the *Weiss-Penzias et al.* [2009] data has a higher amplitude of variation and tends to have a higher absolute value.

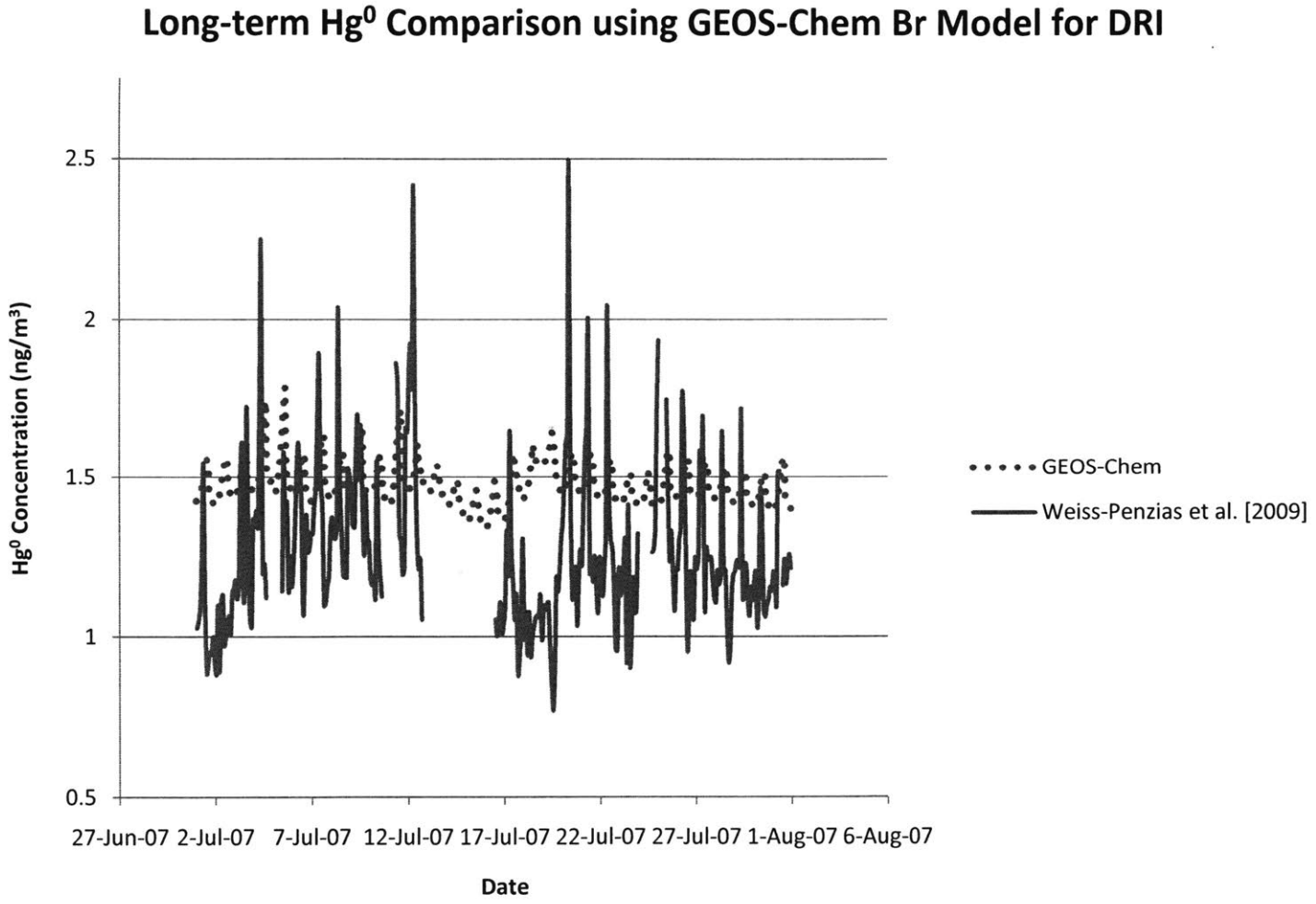

Figure 7. Long-term Hg^0 Comparison using GEOS-Chem Br Model for DRI. The solid line represents data from *Weiss-Penzias et al.* [2009] and the dashed line represents the GEOS-Chem model run data using Br chemistry. Note that the amplitude of variation appears to be larger for the *Weiss-Penzias et al.* [2009] data.

Long-term trends in Hg^0 concentrations would be controlled by elemental gaseous mercury emissions, which are included in GEOS-Chem. DRI and NV98 are in the same GEOS-Chem grid box so they have the same GEOS-Chem values. However, NV98 and DRI have very different local conditions, as was described earlier, which could result in the different mean Hg^0 concentrations. DRI is located in a desert and is near known gold, silver and mercury deposits, which would cause increased Hg^0 levels, and GEOS-Chem may actually be over-predicting these emissions [*Garside and Schilling,* 1979]. GEOS-Chem sees DRI as being in close proximity to anthropogenic emissions, which could also lead to an over-prediction of Hg^0 emissions. Since DRI is at a higher altitude and Hg^0 decreases with altitude, it makes sense that Hg^0 concentrations would be lower compared to the other sites [*Swartzendruber et al.,* 2006]. The average daily means for the GEOS-Chem data and the Nevada measurements are shown in Table 3. The GEOS-Chem data is from the bromine chemistry model run. The means are for the entire three month time period rather than the one month shown in the graphs.

Table 4. Hg^0 Mean Concentrations for GEOS-Chem Br Model and *Weiss-Penzias et al.* [2009] Data. Note that GEOS-Chem under-predicts the Hg^0 concentration for every site except DRI. The means are shown including DRI and not including DRI.

Source	Site	Mean Hg^0 Concentration (ng/m^3)	Difference Below *Weiss-Penzias et al.* [2009] (ng/m^3)
***Weiss-Penzias et al.* [2009]**	NV98	1.674	--
***Weiss-Penzias et al.* [2009]**	NV02	1.763	--
***Weiss-Penzias et al.* [2009]**	DRI	1.254	--
GEOS-Chem	NV98	1.481	0.193
GEOS-Chem	NV02	1.519	0.244
GEOS-Chem	DRI	1.481	-0.227
		MEAN	**0.219 (-DRI), 0.07 (+DRI)**

As shown in the values in Table 4, the Hg^0 concentration tends to be under-predicted by GEOS-Chem for NV02 and NV98. The measured concentration of Hg^0 more closely resembles the nighttime mean Hg^0 concentration of the free troposphere [*Swartzendruber et al.*, 2006]; GEOS-Chem may not capture the free troposphere-boundary layer processes occurring at higher altitudes. As such, the DRI mean difference was not taken into account when determining a mean Hg^0 concentration difference. The mean Hg^0 concentration difference between the Nevada measurements and the GEOS-Chem bromine data was 0.219 ng/m^3, with the Nevada measurements being higher than the GEOS-Chem data. Including DRI, the mean was pushed down to 0.07 ng/m^3.

Increasing the Hg^0 concentration in the model can be accomplished by increasing elemental mercury emissions. An increase in Hg^0 concentrations in the box model of 0.219 ng/m^3 could be achieved by increasing Hg^0 emissions from 30

pg/m^3 hr to 55 pg/m^3 hr, which is well within the emissions range specified by *Coolbaugh et al.* [2002]. Including DRI, an increase of Hg^0 concentrations in the box model of 0.07 ng/m^3 could be achieved by increasing Hg^0 emissions from 30 pg/m^3 hr to 40 pg/m^3 hr, which is also well within the emissions range specified by *Coolbaugh et al.* [2002].

As shown in Figure 8, raising Hg^0 emissions to either 40 or 55pg/m^3 hr in the box model would cause an elemental mercury diurnal trend peaking during the day. This daily trend would be of sufficient magnitude to be measurable in the field. The peak of this signal would be occurring during the day with an afternoon peak due to the diurnal signal of mercury emissions, which is the opposite of the trend predicted by mercury oxidation. This increase in elemental mercury emissions is necessary in the GEOS-Chem model because of its underestimation of the mean elemental mercury concentration. However, note that the initial emissions conditions of the box model (30 pg/m^3 hr) have the correct Hg^0 when compared to the Nevada measurements and that these emissions changes are not necessary for the box model. Note that the sharp decrease in Hg^0 seen in the initial box model run is caused by bromine oxidation. As emissions increase, the decrease becomes less sharp as emissions become more significant in the equation.

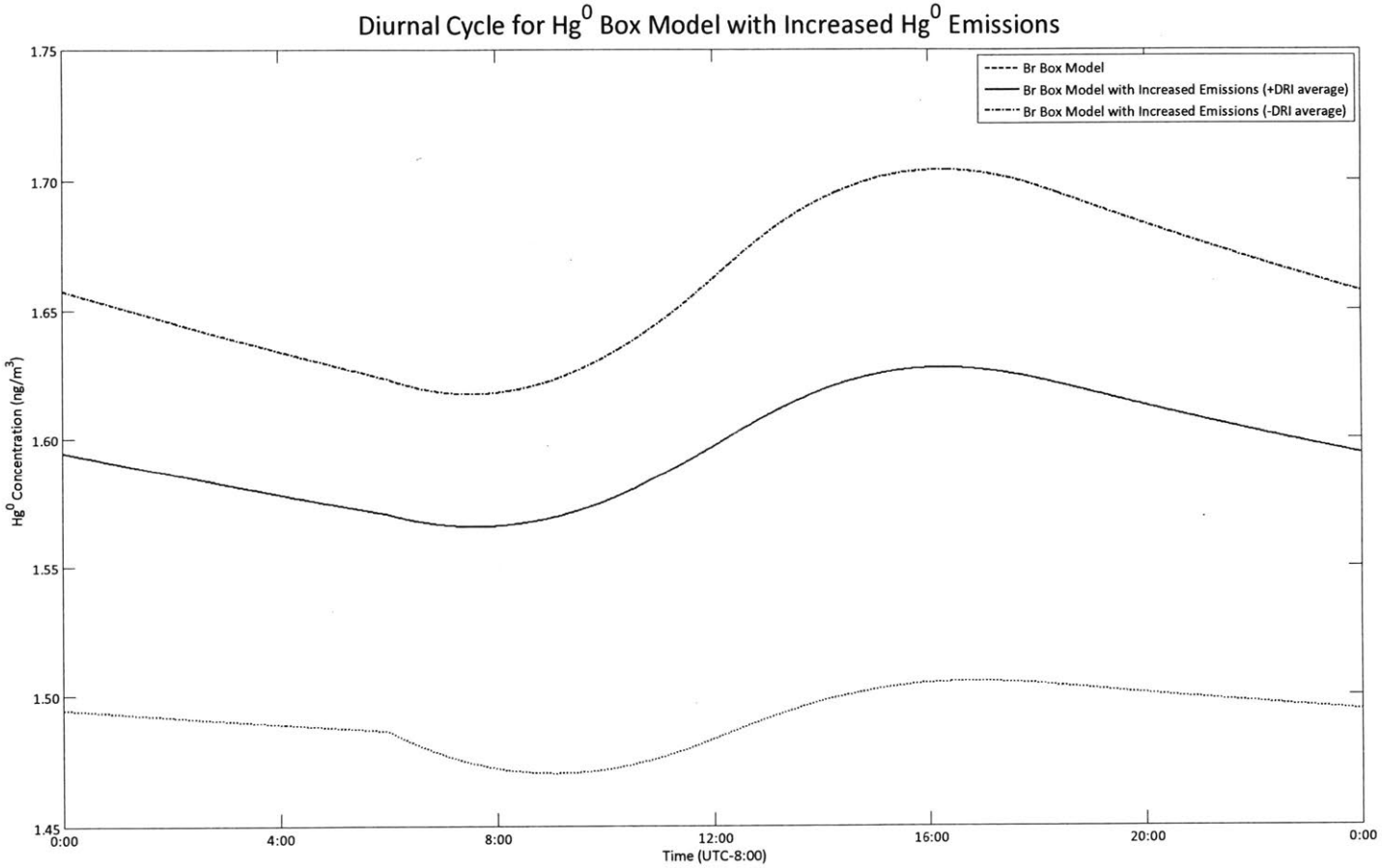

Figure 8. Hg^0 Concentrations with Increased Hg^0 Emissions. The bottom line (red dashed) shows the initial Br Box Model with initial emissions (30 pg/m^3 hr). The middle line (green) shows the diurnal variation of Hg^0 with emissions increased to raise the Hg^0 concentration 0.07 ng/m^3. The top line (blue dashed) shows the diurnal variation of Hg^0 with emissions increased to raise the Hg^0 concentration 0.219 ng/m^3. The peak is so late in the day because the diurnal trend of soil emissions dominates the signal compared to the diurnal signal from oxidation.

4.2 Reactive Gaseous Mercury Diurnal Trends

The amplitude of diurnal variations for Hg^{2+} is too low in GEOS-Chem compared to the *Weiss-Penzias et al.* [2009] data for both oxidation chemistries at all locations, which is shown in Figure 9.

Looking at Figure 9, it is clear that the model runs for GEOS-Chem using OH and Br chemistry both have reactive gaseous mercury diurnal variations that are too small. Br chemistry is considered to be more accurate than OH chemistry for several reasons, including kinematics, mercury residence times, and seasonal mercury cycles [*Holmes et al.,* 2006; *Holmes et al.,* 2010]. The peak timing for both chemistries in the GEOS-Chem model is too late compared to the *Weiss-Penzias et al.* [2009] data. Given that bromine chemistry causes an earlier peak than OH chemistry, bromine chemistry would be the more correct oxidant for this reason as well [*Holmes et al.,* 2010]. The DRI diurnal amplitude was too small by a factor of three. The NV02 diurnal variation was off by a factor of 0.5, meaning that the GEOS-Chem variation was too high; the issues with this site will be discussed shortly. The NV98 diurnal variation was off by a factor of four.

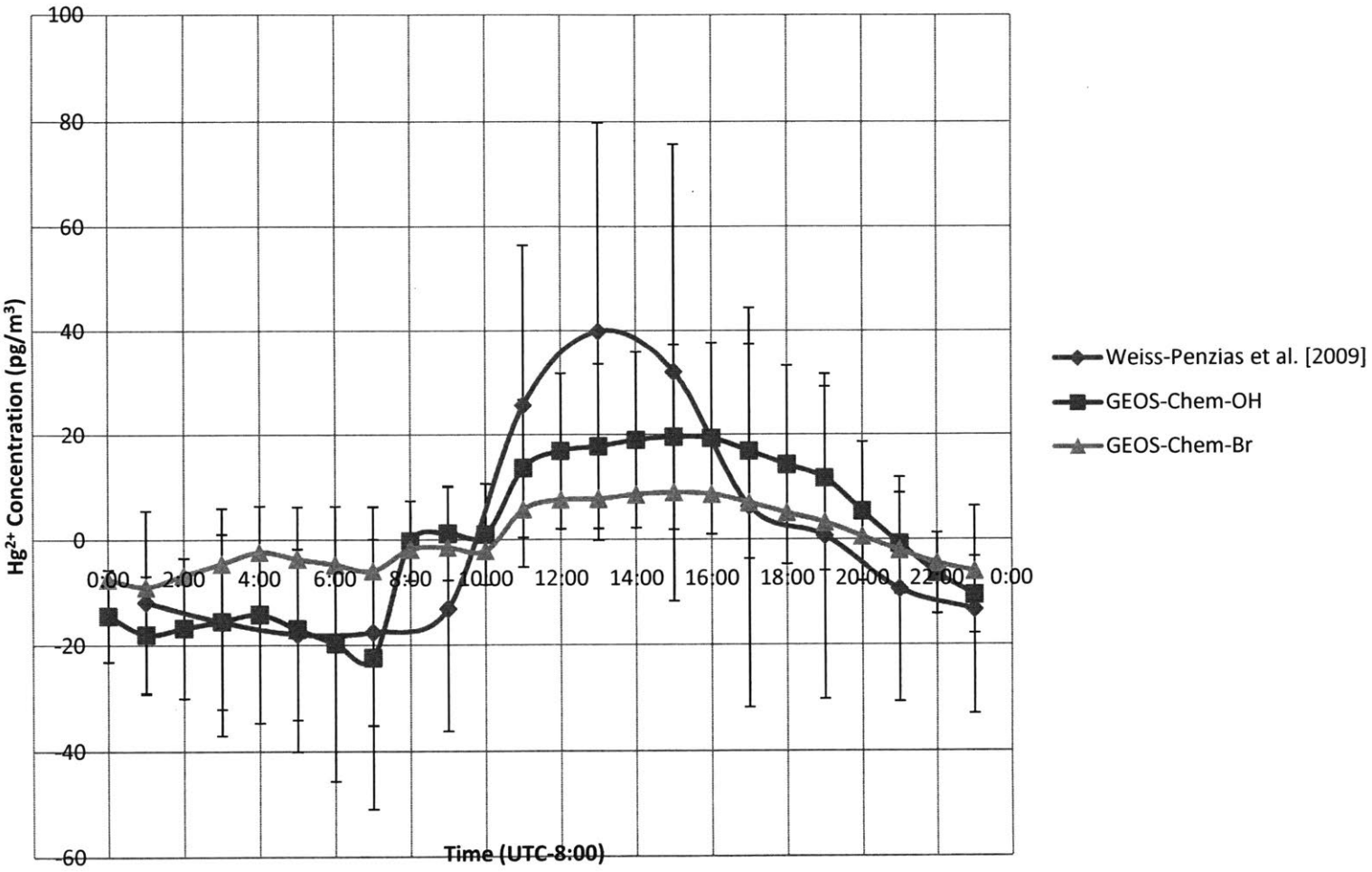

Figure 9. Hg^{2+} Diurnal Variation from the Daily Mean for DRI. The blue–diamond line indicates the *Weiss-Penzias et al.* [2009] data. The red-square line is the GEOS-Chem OH model run. The green triangle line is the GEOS-Chem Br model run. The error bars are ±1 standard deviation. Note that none of the model runs have a high enough diurnal amplitude and that neither model run s peaks during the correct time of day.

Looking at Figure 10, it is clear that the GEOS-Chem model does not accurately represent the chemistry and physics occurring at the NV02 site; reactive gaseous mercury does not follow the trend of peaking during the day. The *Weiss-Penzias et al.* [2009] data follows the predicted diurnal trend and is not affected by the same RGM nighttime peak, meaning that GEOS-Chem has—or does not have—some process actually affecting RGM daily concentrations. This is most likely due to issues with the way the GEOS-Chem grid boxes and local physics are represented. During daylight hours, there is a RGM peak, which can be seen in Figure 10 between 8:00 and 19:00, which could be representative of photochemical oxidation of elemental mercury. However, the concentration of Hg^{2+} increases severally at night, which could possibly be due interactions between the free tropospheric reactive gaseous mercury and reactive gaseous mercury in the boundary layer. Free tropospheric mercury, which was explained earlier in the Methods section, peaks during the night, which could help explain some of this trend [*Swartzendruber et al.,* 2006]. The graph for reactive gaseous mercury for NV98 can be found in Appendix 3 and was not significantly different from the DRI graph.

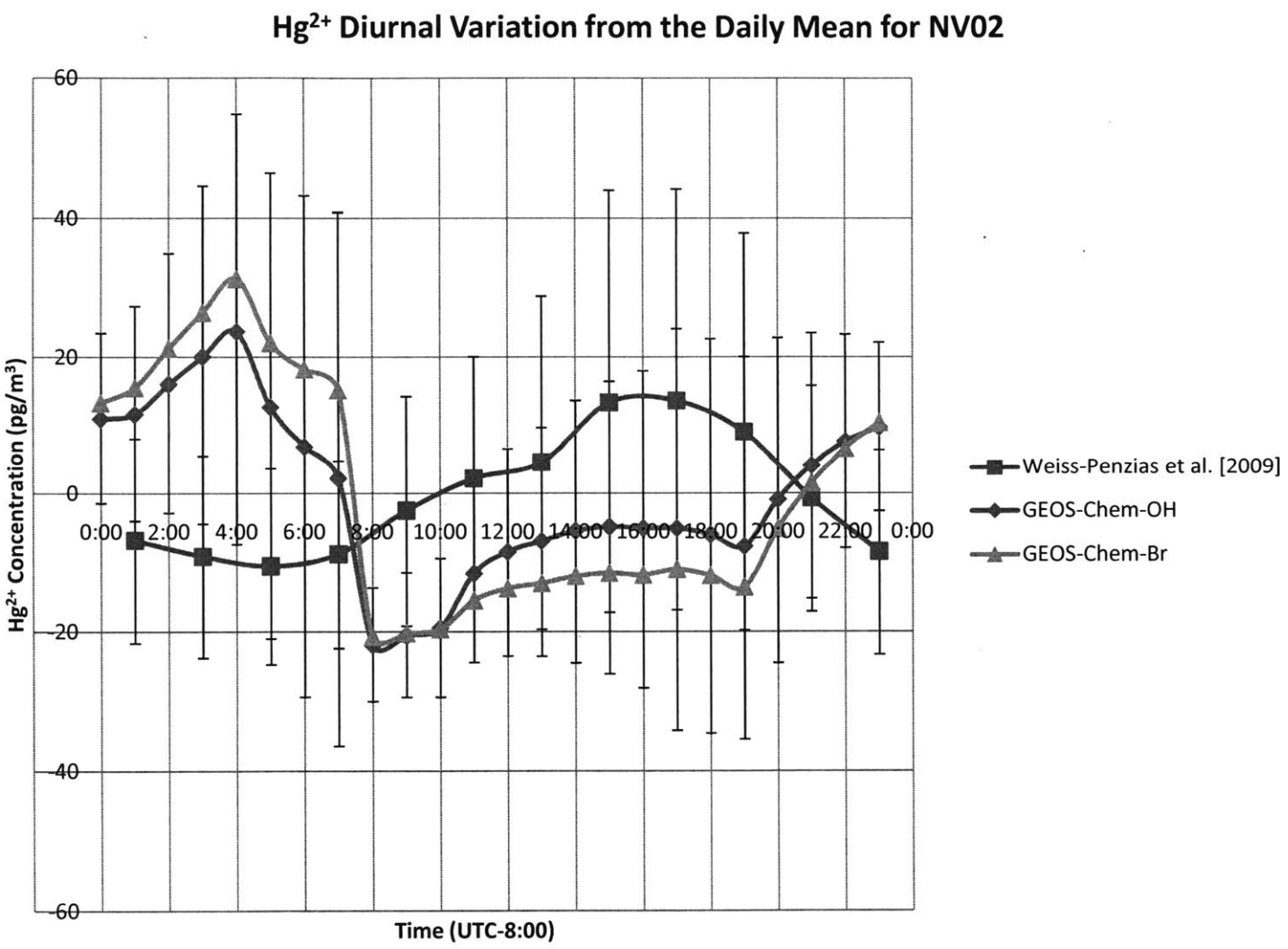

Figure 10. Hg^{2+} Diurnal Variation from the Daily Mean for NV02. The blue–diamond line indicates the GEOS-Chem OH model run. The red-square line is the *Weiss-Penzias et al.* [2009] data. The green triangle line is the GEOS-Chem Br model run. The error bars are ±1 standard deviation. Note that none of the model runs have a high enough diurnal amplitude and that neither model run peaks during the correct time of day. Also note the rather bizarre diurnal trend at this site.

Given the diurnal nature of the errors and the previous description of free and constrained parameters, there are several parameters that could control diurnal variation of RGM. These include emissions, oxidation, RGM dry deposition, and entrainment. As mentioned earlier, RGM may be emitted, which will also be discussed. These factors will be tested using the box model described in the Methods section. The initial run of the box model—using values listed in the Methods section—is shown in Figure 11. For completeness sake, the model was also run using OH chemistry parameters [*Lin et al.,* 2006; *Selin et al.,* 2007; *Seigneur and Lohman,* 2008]. Note that in Figure 11, the OH peak timing is too late in the day compared to the *Weiss-Penzias et al.* [2009] DRI data, while the Br peak timing is more accurate. The analyses here were done using the DRI *Weiss-Penzias et al.* [2009] data; initial box model runs compared to NV98 and NV02 data can be found in Appendix 3. The box model appears to represent NV02 better than NV98 due to the smaller diurnal amplitude in the NV02 data.

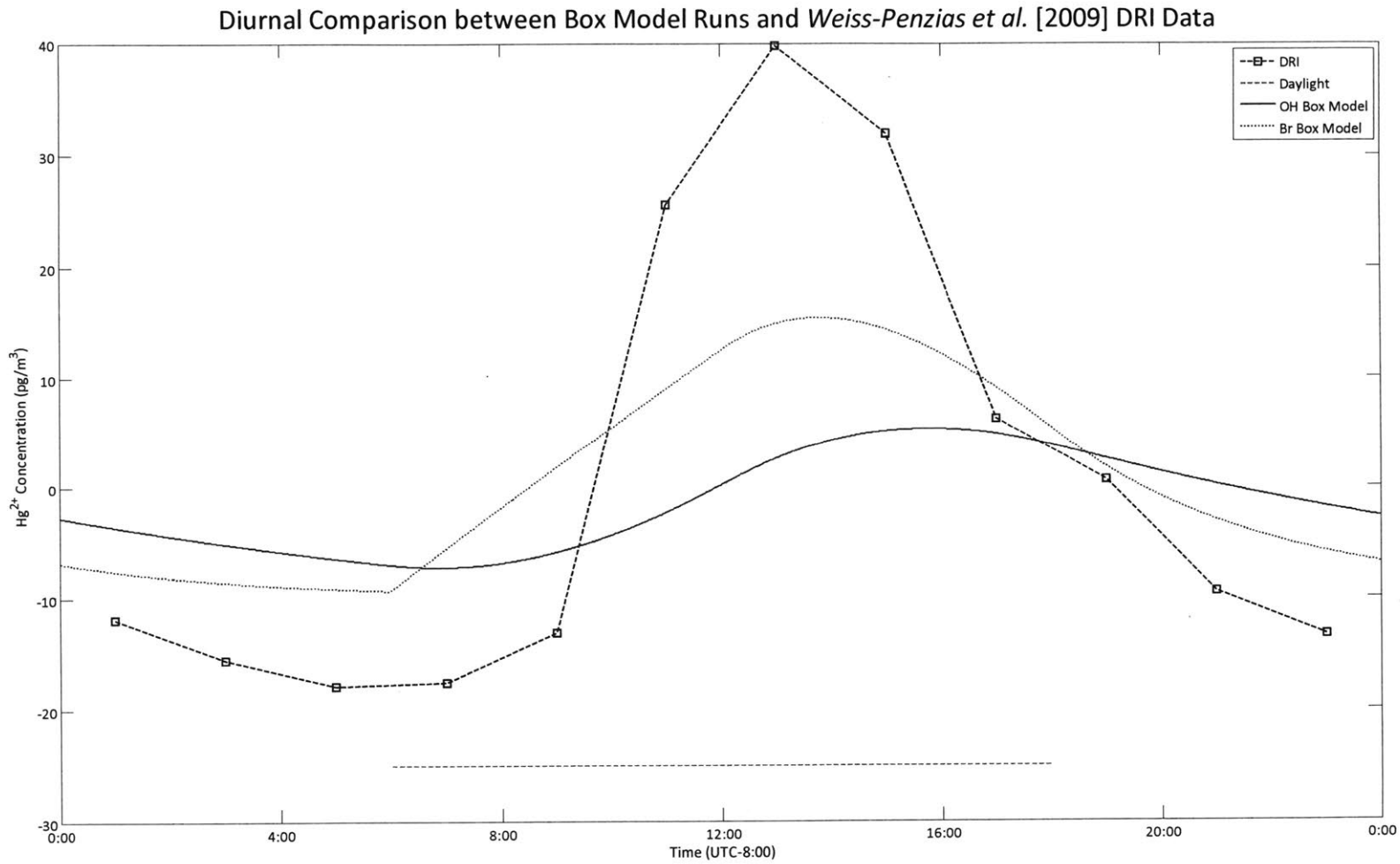

Figure 11. Diurnal Comparison between Box Model Runs and *Weiss-Penzias et al.* [2009] DRI Data. The blue square dashed line shows the DRI variations from the mean. The solid green line shows the OH box model run. The red dashed line shows the Br box model run. The orange dashed line indicates daylight hours. This graph shows hourly variations from the daily mean.

4.2.1 Elemental Mercury Emissions

Changing mercury emissions could result in the desired diurnal variations for reactive gaseous mercury. Increasing both elemental and reactive gaseous mercury emissions could cause the increase in diurnal variations from the mean because of the diurnal cycle of emissions, but only elemental mercury emissions are discussed in this section.

Increasing elemental mercury emissions would cause an increase in the diurnal cycle of reactive gaseous mercury due to the relationship between Hg^0 and Hg^{2+} concentrations, as can be seen in Equations 2 and 3 on page 46 in the Methods section. Through trial and error using the bromine chemistry version of the box model, elemental mercury emissions would need to increase to 25 times initial emissions levels to cause the observed diurnal amplitude for reactive gaseous mercury, which can be seen in Figure 12. This would be an increase from 30 pg/m^3 hr to 750 pg/m^3 hr, which far exceeds the highest values proposed by *Coolbaugh et al.* [2002]. As mentioned earlier, since emissions of even 55 pg/m^3 hr would cause an increased, incorrect diurnal signal in elemental mercury (see Figure 8), increasing elemental mercury emissions would not be able to completely resolve the diurnal variation amplitude issues of GEOS-Chem [*Holmes et al.*, 2009; *Weiss-Penzias et al.*, 2009].

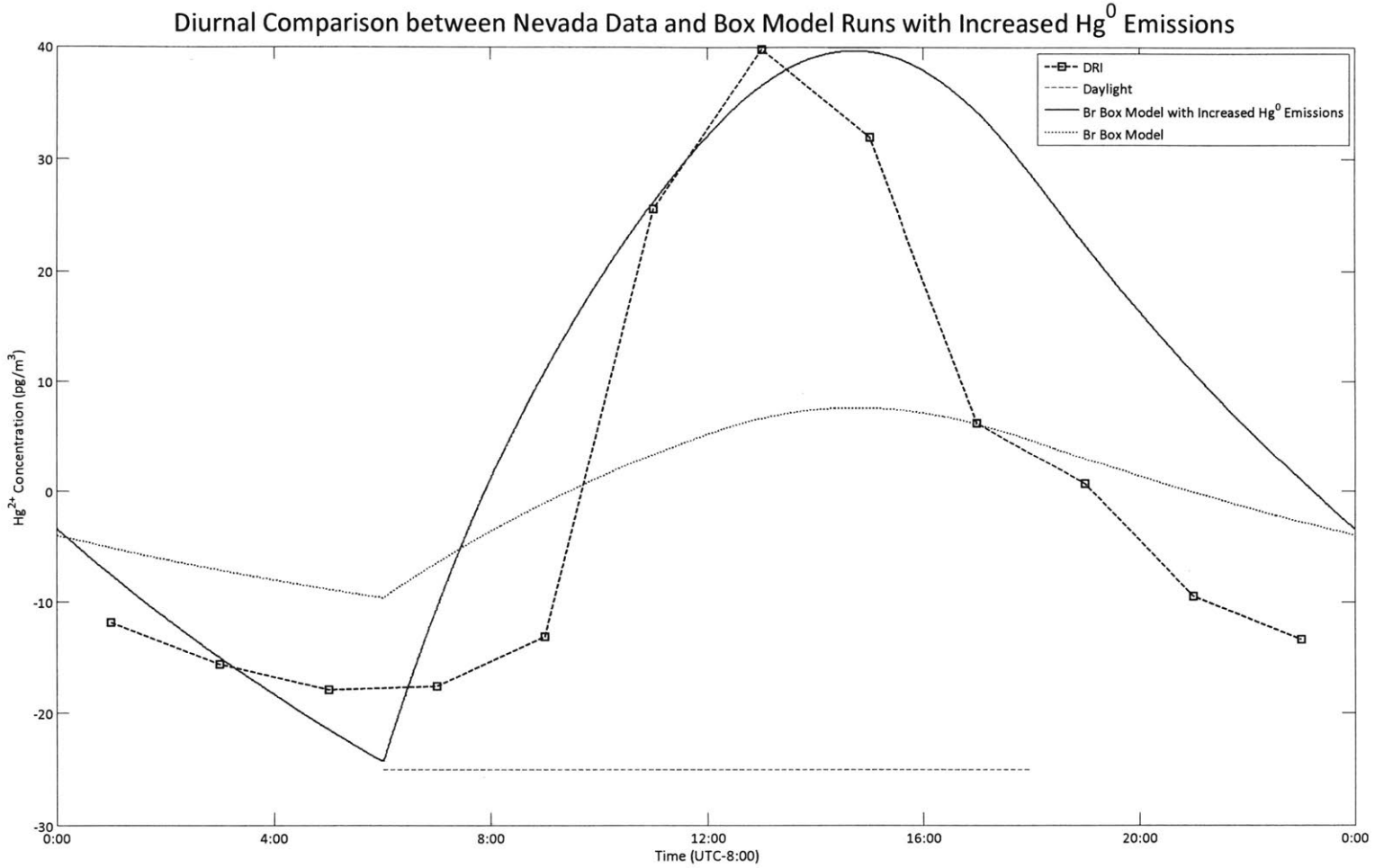

Figure 12. Diurnal Comparison between Nevada Data and Box Model Runs with Increased Hg^0 Emissions. The blue square dashed line shows the DRI variations from the mean. The red dashed line shows the initial Br box model run. The orange dashed line indicates daylight hours. The green solid line show RGM levels with Hg^0 emissions 25 times higher than initial values. This graph shows hourly variations from the daily mean.

4.2.2 Oxidation

Changing the rate of oxidation or the concentration of the oxidant would also serve to increase diurnal variations because of the diurnal nature of photochemical oxidation.

Through trial and error using the bromine chemistry box model, it was determined that multiplying the oxidation term, $k \times [oxidant] \times [c]$, by a factor of 5 was enough to cause the observed diurnal variations (see Figure 13). This value could be applied to the rate constant or the concentration of bromine. However, the rate constants remain the same over the three sites, so differences in diurnal variations between the three sites would be the result of changes in the concentration of the oxidant. Given that the rate constant is already near the edge of its range, its value would not change [*Holmes et al.,* 2006; *Seigneur and Lohman,* 2008; *Holmes et al.,* 2010]. Given that the initial concentration of bromine in the box model was on the low end of an atmospheric range that varied by orders of magnitude, an increase by a factor of five would be completely reasonable [*Seigneur and Lohman,* 2008].

Note that when oxidation levels are increased, the oxidation term becomes more significant in the box model, thus shifting the Hg^{2+} peak in the day to more

closely match the observed DRI peak, which can be seen in Figure 13. This is due to the daily profile of bromine (Figure 4).

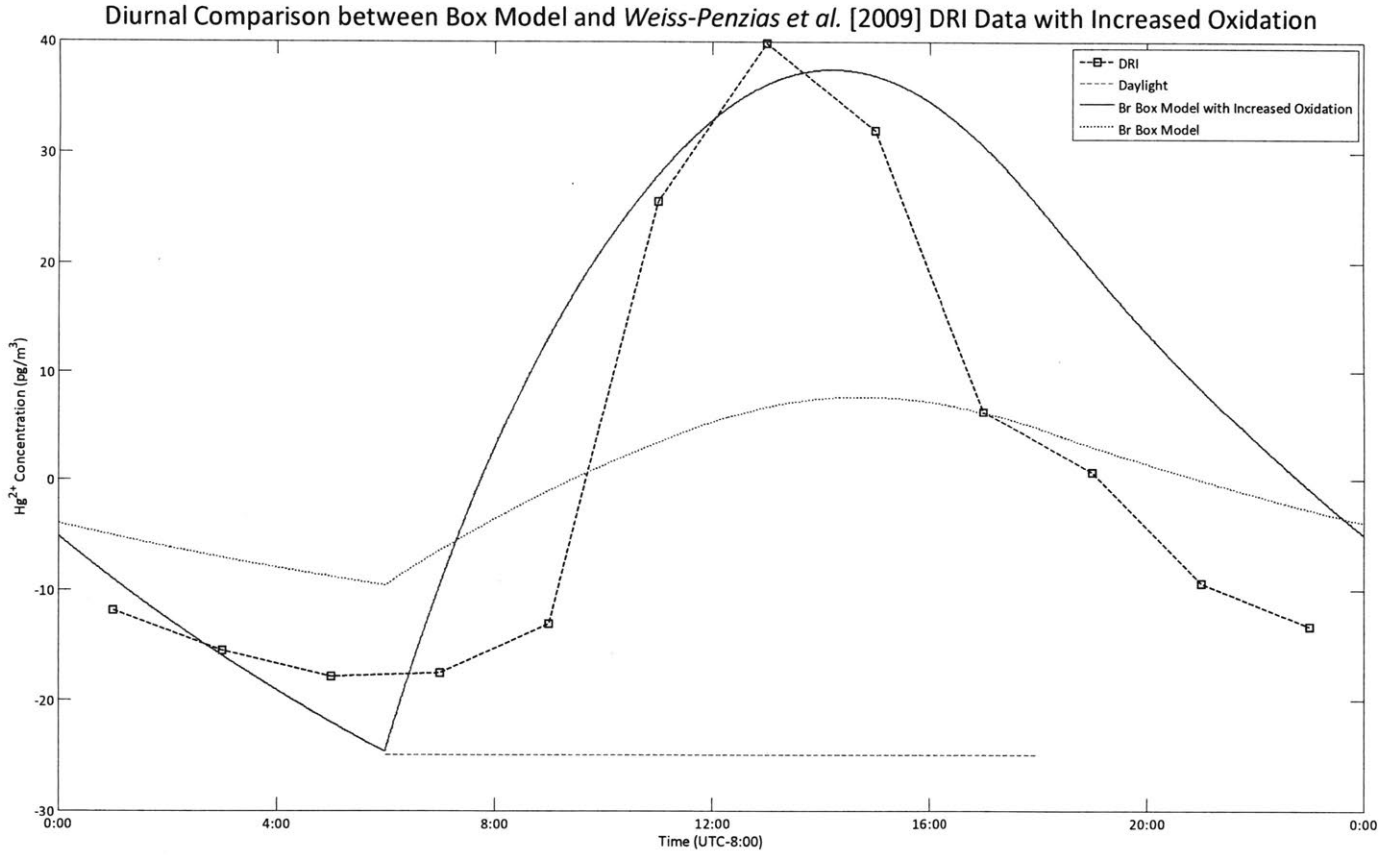

Figure 13. Diurnal Comparison between Box Model and *Weiss-Penzias et al.* [2009] DRI Data with Increased Oxidation. The blue square dashed line shows the DRI variations from the mean. The red dashed line shows the initial Br box model run. The orange dashed line indicates daylight hours. The green solid line show RGM levels with the oxidation term multiplied by 5. This graph shows hourly variations from the daily mean.

4.2.3 Reactive Gaseous Mercury Dry Deposition

Pushing the reactive gaseous mercury dry deposition velocity to the maximum of its range at 6 cm/s (or 216 m/hr) over the initial velocity of 1 cm/s (or 36 m/hr) does not cause enough of a diurnal variation to match the DRI data, as can be seen in Figure 14 [*Zhang et al.*, 2009]. The initial value was chosen because of the type of land in the *Weiss-Penzias et al.* [2009] study. Also, the change in dry deposition velocity shifts the timing of the RGM peak, but actually reduces the diurnal variability. As such, increasing dry deposition rates serves to damp out some of the RGM diurnal signal.

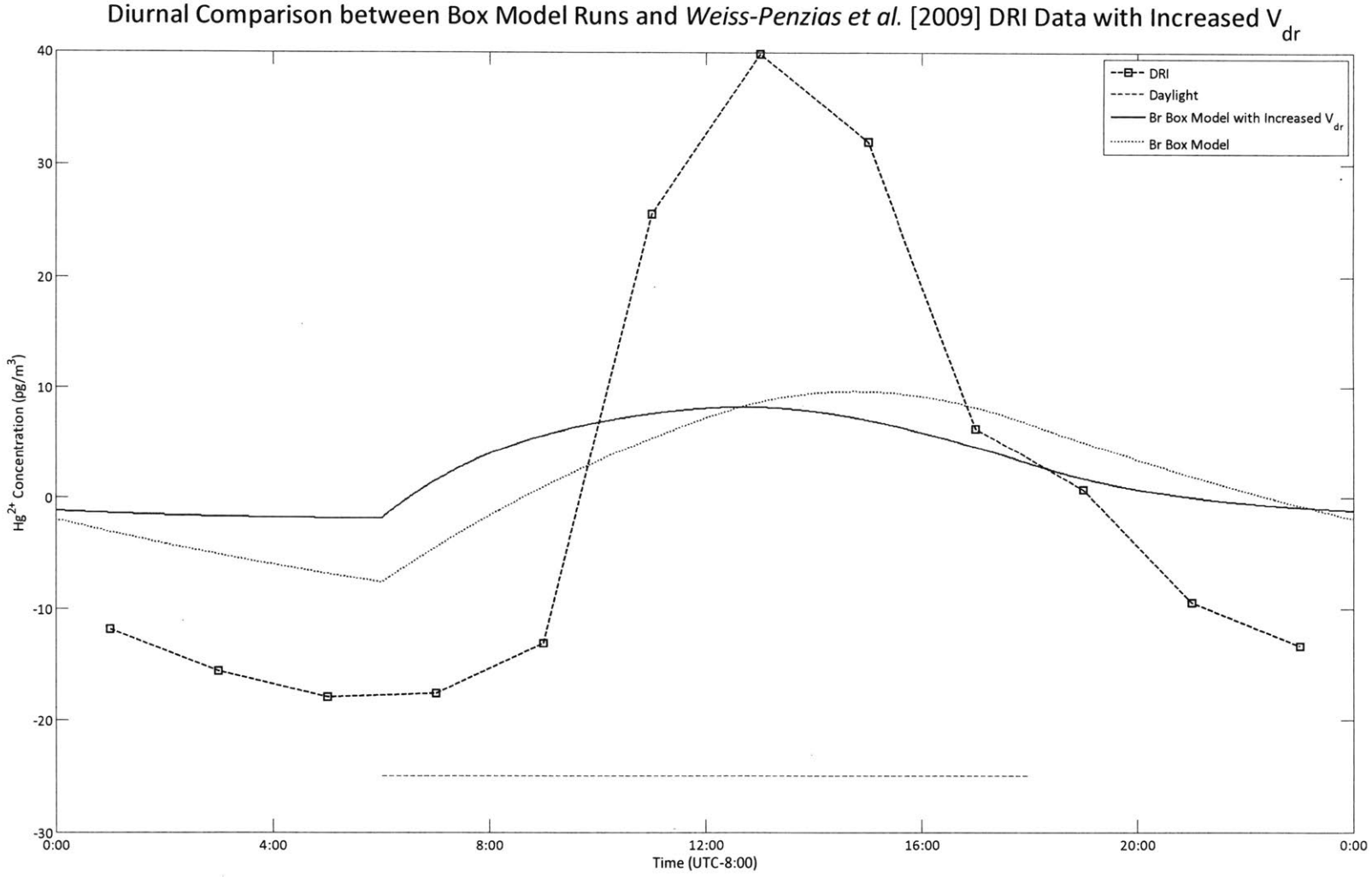

Figure 14. Diurnal Comparison between Box Model and *Weiss-Penzias et al.* [2009] DRI Data with Increased v_{dr}. The blue square dashed line shows the DRI variations from the mean. The red dashed line shows the initial Br box model run. The orange dashed line indicates daylight hours. The green solid line show RGM levels with the RGM dry deposition velocity is increased to the maximum of its range, 6 cm/s. This graph shows hourly variations from the daily mean.

4.2.4 Entrainment

As mentioned earlier, RGM entrainment follows a diurnal trend based on the concentration of Hg^{2+} in the free troposphere. In the initial run of the box model, the concentration of reactive gaseous mercury in the free troposphere was allowed to fluctuate between 43 pg/m^3 and 66 pg/m^3 over the course of the day in the model runs, which is consistent with average values from *Swartzendruber et al.* [2006]. The maximum amplitude of diurnal variation was observed to be 600 pg/m^3 [*Swartzendruber et al.,* 2006]. Figure 15 shows the diurnal trend of reactive gaseous mercury variation in the free troposphere increased to allow for a daily fluctuation between 43 pg/m^3 and 600 pg/m^3. Note that the diurnal amplitude of the box model is the correct size for the *Weiss-Penzias et al.* [2009] DRI data. However, the RGM peak is still too late in the day.

Other studies have shown that the maximum enhancement is only on the order of 140 pg/m^3 rather than the 600 pg/m^3 used here [*Faïn et al.,* 2009]. Enhancements this large were not seen every day during the study, meaning that they are relatively rare events and would not be solely capable of causing the average diurnal amplitude seen in the *Weiss-Penzias et al.* [2009] data [*Swartzendruber et al.,* 2006].

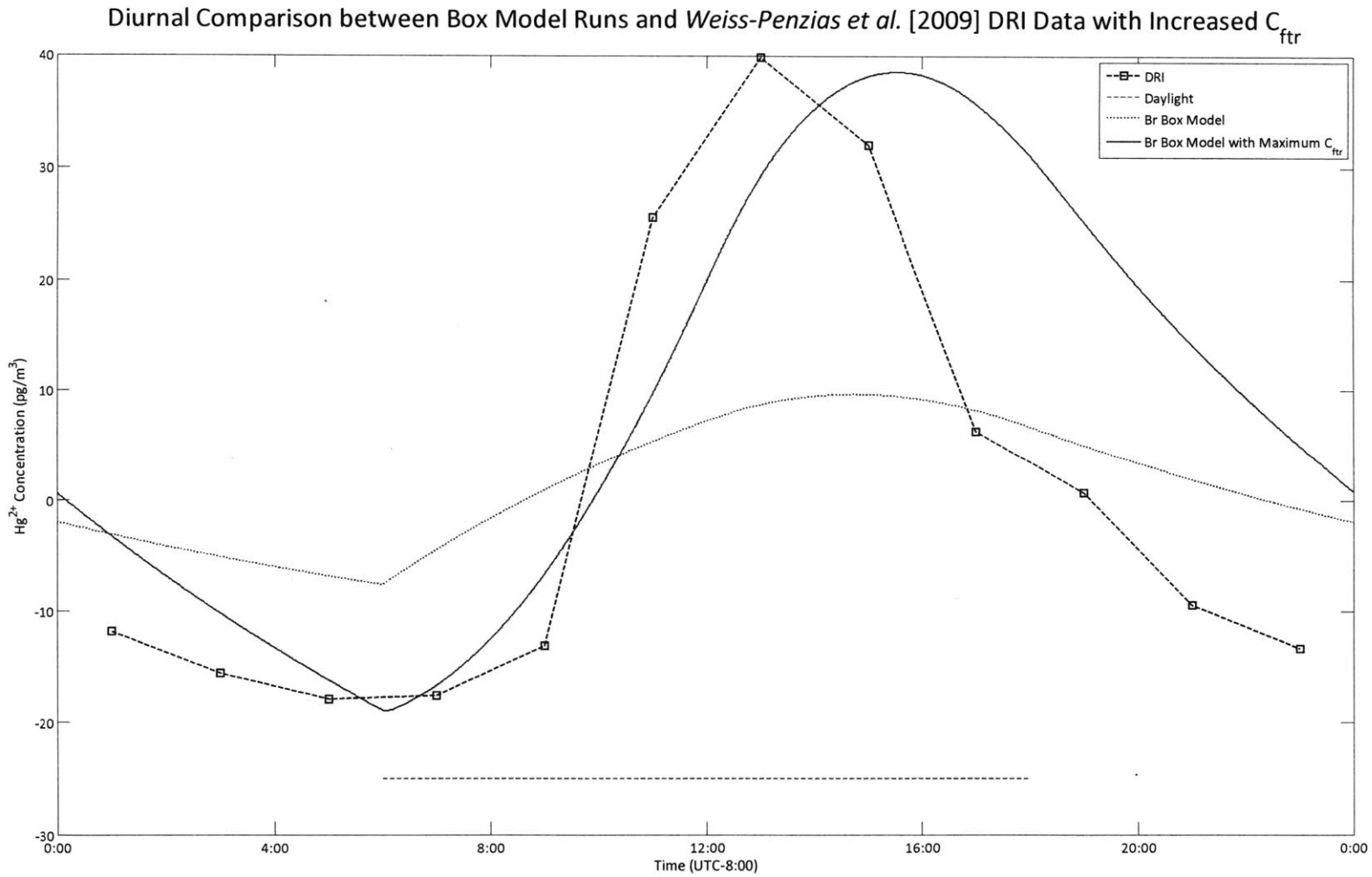

Figure 15. Diurnal Comparison between Box Model and *Weiss-Penzias et al.* [2009] DRI Data with Increased C_{ftr}. The blue square dashed line shows the DRI variations from the mean. The red dashed line shows the initial Br box model run. The orange dashed line indicates daylight hours. The green solid line show RGM levels with concentration of RGM allowed to reach 600 pg/m^3 in the free troposphere. This graph shows hourly variations from the daily mean.

4.2.5 Reactive Gaseous Mercury Emissions

Increasing reactive gaseous mercury emissions would also increase the diurnal variation of Hg^{2+}, provided that Hg^{2+} emissions follow a diurnal pattern and are actually occurring. As mentioned earlier, reactive gaseous emissions are thought to only comprise up to 5% of total emissions, which would be 1.5 pg/m^3 hr considering that elemental mercury emissions, which would make up 95% of emissions, are 30 pg/m^3 hr [*Gustin,* 2003]. Alternatively, reactive gaseous emissions are thought to comprise 50% of anthropogenic emissions, which are 2 pg/m^3 hr in the model, resulting in a RGM emission component of 1 pg/m^3 hr. Both emissions regimes are shown in Figure 16. As can be seen, neither set of emissions regimes contributes significantly to the diurnal amplitude of Hg^{2+} concentrations; nor do they move the RGM peak to correct time of day.

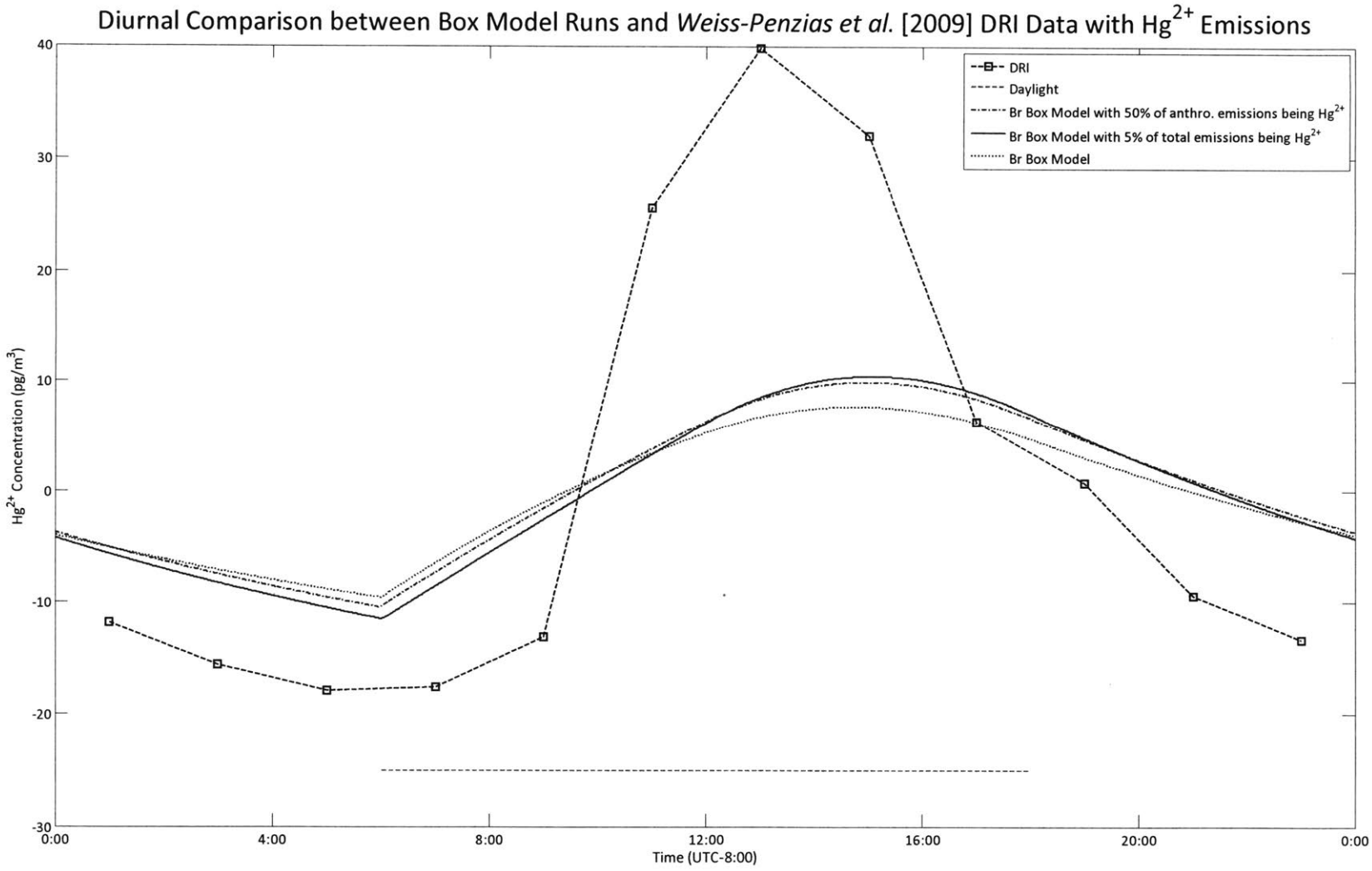

Figure 16. Diurnal Comparison between Box Model and *Weiss-Penzias et al.* [2009] DRI Data with Hg^{2+} Emissions. The blue square dashed line shows the DRI variations from the mean. The red dashed line shows the initial Br box model run. The orange dashed line indicates daylight hours. The green solid line shows RGM levels with Hg^{2+} emissions comprising 5% of total emissions. The green dashed line shows RGM levels with Hg^{2+} emissions comprising 50% of anthropogenic emissions. This graph shows hourly variations from the daily mean.

4.2.6 Reasonable Changes

Considering that none of the processes occurring the atmosphere happen in isolation, changes in oxidation and free tropospheric mercury concentrations could result in a profile similar to the observed DRI without drastic changes in any one quantity. Figure 17 shows the diurnal profile with those combined changes. Given that the initial box model run estimated the correct elemental mercury mean concentration, elemental mercury emissions were not changed here.

Oxidation was increased by a factor of 4, which could be applied to the concentration of bromine. Given uncertainties in the bromine concentration over different land types, this increase could even be on the low side of actual increases [*Seigneur and Lohman,* 2008]. The RGM dry deposition velocity was not increased because the original value of 36 m/hr was chosen due to the desert location of the *Weiss-Penzias et al.* [2009] sites and increases only served to reduce the diurnal RGM signal. The concentration of RGM in the free troposphere was allowed to fluctuate up to 110 pg/m^3 rather than the original 66 pg/m^3. The changes are summarized in Table 5.

Table 5. Reasonable Changes to Parameters. This table shows the initial values for parameters as well as the values of the parameters after they were changed.

Parameter	Initial	Changed
Oxidation	$2.75\times10^{-3} \times [c_e]$ pg/m^3	$1.1\times10^{-2} \times [c_e]$ pg/m^3
C_{ftr} **Fluctuation**	up to 66 pg/m^3	up to 110 pg/m^3

Figure 17 shows the diurnal variation for DRI with these changes. Note that the RGM peak occurs at a more realistic time of day and that the decreasing behavior in the pre-dawn hours is quite similar. However, also note that the RGM peak is much broader for the box model compared to the Nevada measurements.

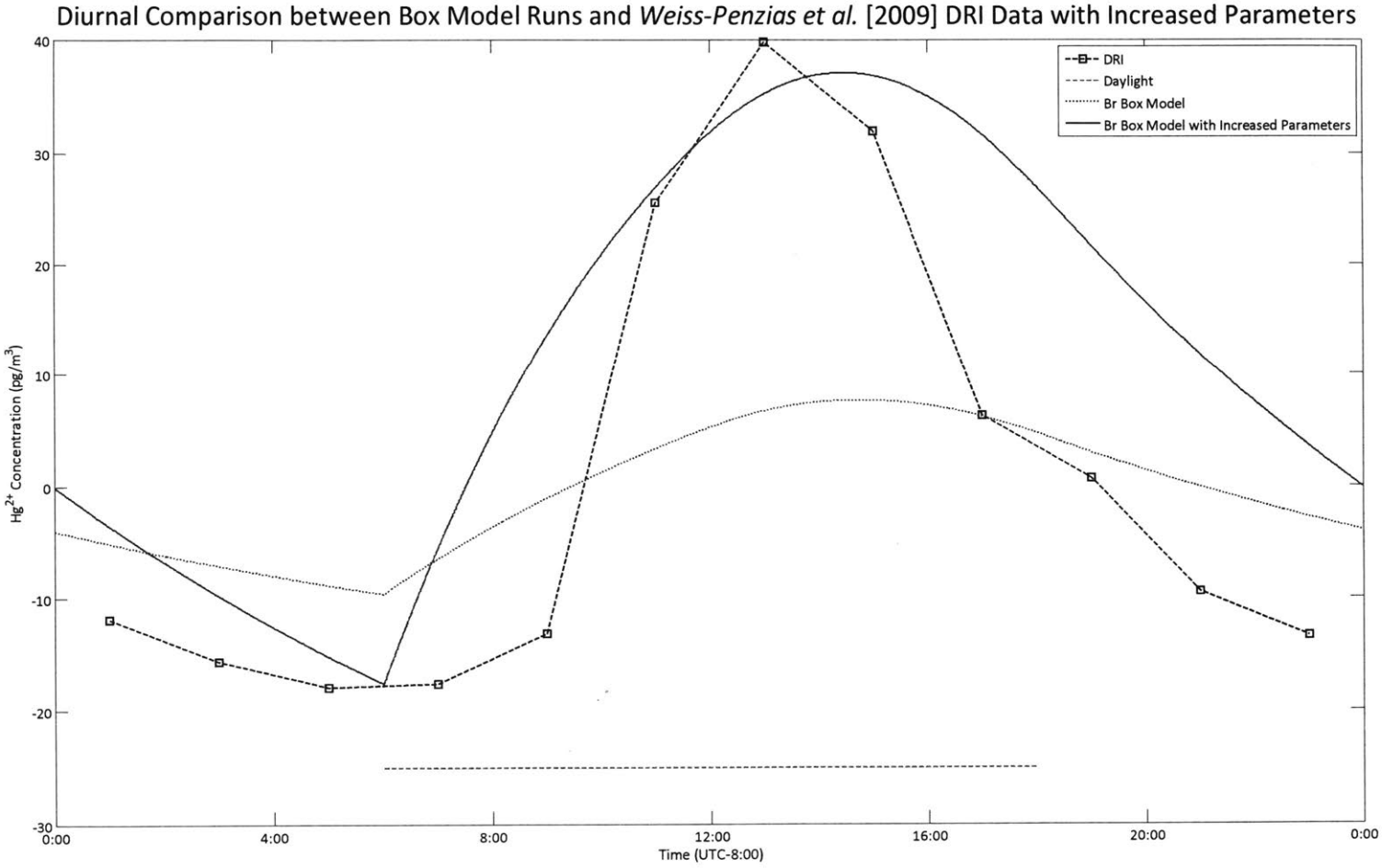

Figure 17. Diurnal Comparison between Box Model and *Weiss-Penzias et al.* [2009] DRI Data with Increased Parameters. The blue square dashed line shows the DRI variations from the mean. The red dashed line shows the initial Br box model run. The orange dashed line indicates daylight hours. The green solid line shows the Br box model run with increased parameters. This graph shows hourly variations from the daily mean.

5. CONCLUSIONS

Based on the comparisons made between the GEOS-Chem model runs and data from *Weiss-Penzias et al.* [2009], it is clear that there are several inconsistencies between the physics and chemistry of the GEOS-Chem model and the actual physics and chemistry of the atmosphere. The major differences include an underestimation of elemental mercury deposition, a reduced diurnal amplitude, and a peak in reactive gaseous mercury occurring at the wrong time of day. Given the processes occurring in the atmospheric mercury cycle, it was determined that the model errors were in photochemical oxidation, elemental mercury emissions, and the fluctuations of the free tropospheric reactive gaseous mercury concentration

Through the use of a box model, it was determined that increasing GEOS-Chem elemental mercury emissions on the order of 10-25 pg/m^3 hr would be necessary to increase elemental mercury mean concentrations, which is well within emissions ranges [*Coolbaugh et al.,* 2002]. However, increases in elemental mercury emissions would start to disrupt the Hg^0 diurnal signal.

Errors in the GEOS-Chem model were also found in the diurnal amplitude of reactive gaseous mercury concentrations, which was caused by a misrepresentation of oxidation and reactive gaseous mercury entrainment.

Combining these parameters, oxidation would need to increase by a factor of 4, which would be applied to the concentration of bromine. This increase is very reasonable considering the range of bromine concentrations in the atmosphere [*Seigneur and Lohman,* 2008]. This increase was also needed in order to shift the RGM peak to the observed time of day. The peak concentration of RGM in the free troposphere would have to increase by a factor of 1.7, which is high considering that although values this high were measured, they occurred rather sparingly [*Swartzendruber et al.,* 2006].

Given the uncertainty in this study, more research needs to be done to understand reactive gaseous mercury emissions, oxidation, and HgP partitioning. Too much is unknown about rural emissions, naturally enhanced mercury patterns, the percentage of mercury emissions that are reactive gaseous mercury, and the diurnal variability of reactive gaseous mercury emissions. Given that so many of these processes occur on very small scales, being able to better parameterize—or parameterize at all—RGM mercury emissions in the GEOS-Chem model would be beneficial. Also, more research focused on oxidation rates and oxidant concentrations is needed to help improve the modeled diurnal amplitude of RGM as well as the time of day that RGM peaks. As mentioned briefly earlier, HgP partitioning is not well understood and represents a potentially large uncertainty in reactive gaseous mercury deposition.

A better understanding of mercury chemistry and physics can help paint a more accurate picture of the global biogeochemical mercury cycle. By understanding the exact nature of mercury transport and deposition, policymakers can make regulatory decisions that will result in the optimal amount of mercury control, thereby reducing mercury exposure and its toxic effects.

APPENDIX 1. BOX MODEL CODE

```
function dcdt=mercury(t,c)

% This is a box model that quantifies dry deposition of mercury over
% land. It includes photochemical oxidation, entrainment from the free
% troposphere, deposition to the ground, and emissions.

dcdt=zeros(2,1);

tnew=rem(t,24);
%Calculate the hour of the day from seconds
%Sun needs to be scaled depending on if the concentrations involved are
%maximum concentrations or not
if (tnew<6)
    sun=0;
elseif (6<tnew && tnew <12)
    sun=1*(tnew-6);
elseif (12<=tnew && tnew<18)
    sun=6e0-(1*(tnew-12));
elseif (tnew>=18)
    sun=0;
end


%Bromine profile
if (tnew<6)
    Br=0;
elseif (6<=tnew && tnew<18)
    Br=12+(6-tnew);
elseif (tnew>=16)
    Br=0;
end

% First column/equation is Hg0
% Second column/equation is Hg+2

%VARIABLES

ve=18;          %entrainment velocity (in m hr^-1)
cfte=1540;      %concentration in the free troposphere (in pg m^-3)
cftr=43;        %concentration in the free troposphere (in pg m^-3)
vde=3.6;        %dry deposition velocity for elemental mercury (in m hr^-1)
vdr=36;         %dry deposition velocity for RGM(in m hr^-1)
z=750;          %boundary layer height (in m)
k=5.5*10^-15;   %rate constant (in m^3 hr^-1 pg^-1)
ox=5*10^11;     %maximum concentration of oxidant (pg m^-3)
Ee=30;          %elemental mercury emissions (pg m^-3 hr^-1)

%EQUATIONS

dcdt(1)=-k*c(1)*Br/12*ox+Ee*sun/6+(ve/z)*(cfte-c(1))-(vde/z)*c(1);
dcdt(2)=k*c(1)*Br/12*ox+(ve/z)*(cftr*sun/4-c(2))-(vdr/z)*c(2);

% run with [t,y]=ode15s('mercury',[0:0.01:240],[1750 25]);
```

```
function dcdt=ozone(t,c)

% This is a box model that tries to quantify dry deposition of mercury over
% land. It includes photochemical oxidation, entrainment from the free
% troposphere, deposition to the ground, and emissions.

dcdt=zeros(2,1);

tnew=rem(t,24);
%Calculate the hour of the day from seconds
%Sun is divided by 3 in the equations to account for lack of information as
%to the time of oxidant measurements
if (tnew<6)
    sun=0;
elseif (6<tnew && tnew <12)
    sun=1*(tnew-6);
elseif (12<=tnew && tnew<18)
    sun=6e0-(1*(tnew-12));
elseif (tnew>=18)
    sun=0;
end

% First column/equation is Hg0
% Second column/equation is Hg+2

%VARIABLES

ve=18;          %entrainment velocity (in m hr^-1)
cfte=1540;      %concentration in the free troposphere (in pg m^-3)
cftr=43;        %concentration in the free troposphere (in pg m^-3)
vde=3.6;        %dry deposition velocity for elemental mercury (in m hr^-1)
vdr=36;         %dry deposition velocity for RGM(in m hr^-1)
z=750;          %boundary layer height (in m)
k=2.56*10^-16;  %rate constant (in m^3 hr^-1 pg^-1)
ox=1*10^12;     %concentration of oxidant (pg m^-3)
Ee=30;          %elemental mercury emissions (pg m^-3 hr^-1)

%EQUATIONS

dcdt(1)=-k*c(1)*sun*ox+Ee*sun/6+(ve/z)*(cfte-c(1))-(vde/z)*c(1);
dcdt(2)=k*c(1)*sun*ox+(ve/z)*(cftr*sun/4-c(2))-(vdr/z)*c(2);

% run with [t,y]=ode15s('ozone',[0:0.01:240],[1750 25]);
```

APPENDIX 2. LONG-TERM COMPARISON GRAPHS

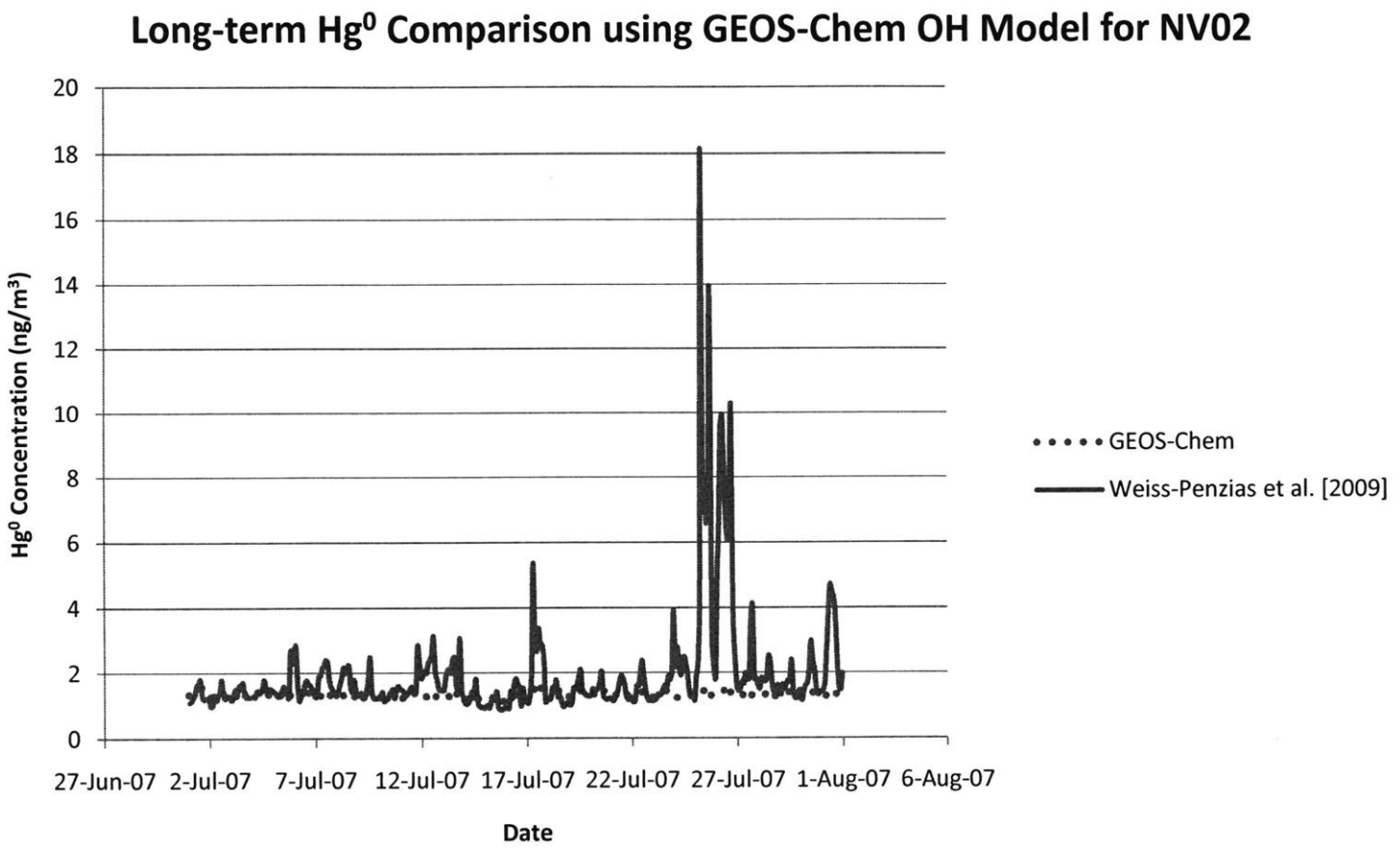

Long-term Hg^0 Comparison using GEOS-Chem OH Model for NV02. The solid line represents data from *Weiss-Penzias et al.* [2009] and the dashed line represents the GEOS-Chem model run data using OH chemistry. Also note that the amplitude of variation appears to be larger for the *Weiss-Penzias et al.* [2009] data.

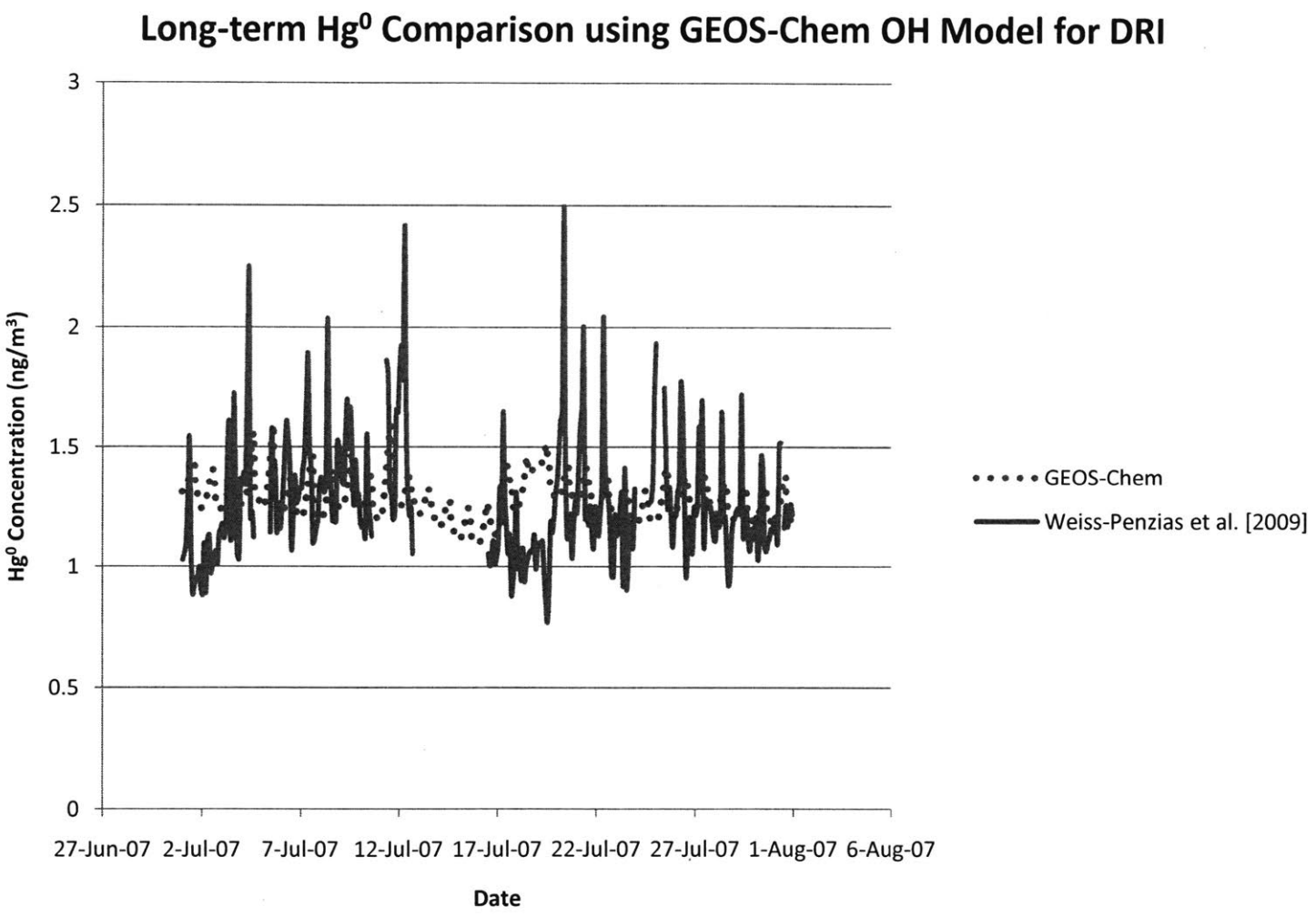

Long-term Hg^0 Comparison using GEOS-Chem OH Model for DRI. The solid line represents data from *Weiss-Penzias et al.* [2009] and the dashed line represents the GEOS-Chem model run data using OH chemistry. Also note that the amplitude of variation appears to be larger for the *Weiss-Penzias et al.* [2009] data.

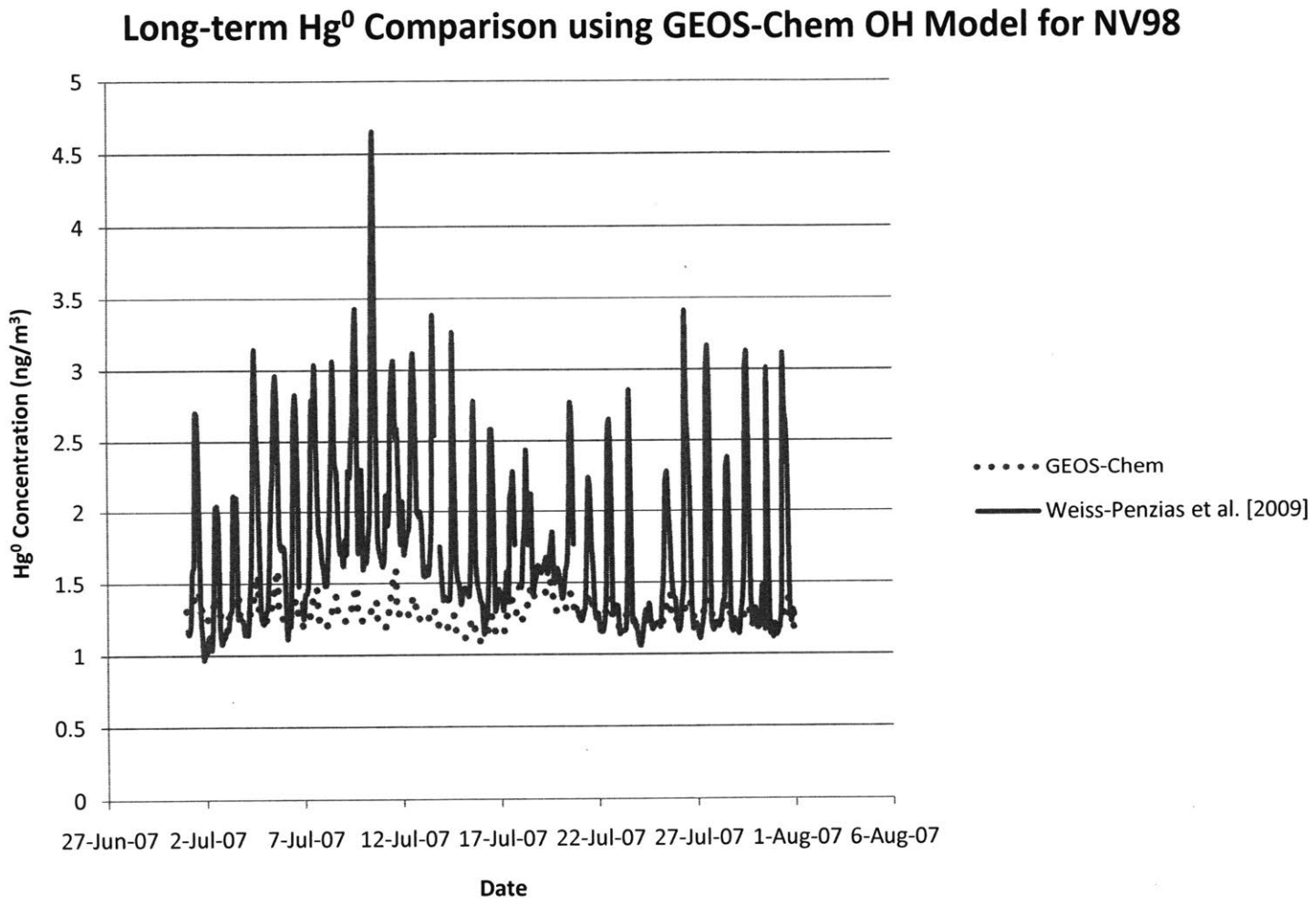

Long-term Hg^0 Comparison using GEOS-Chem OH Model for NV98. The solid line represents data from *Weiss-Penzias et al.* [2009] and the dashed line represents the GEOS-Chem model run data using OH chemistry. Also note that the amplitude of variation appears to be larger for the *Weiss-Penzias et al.* [2009] data.

APPENDIX 3. DIURNAL VARIATION GRAPHS

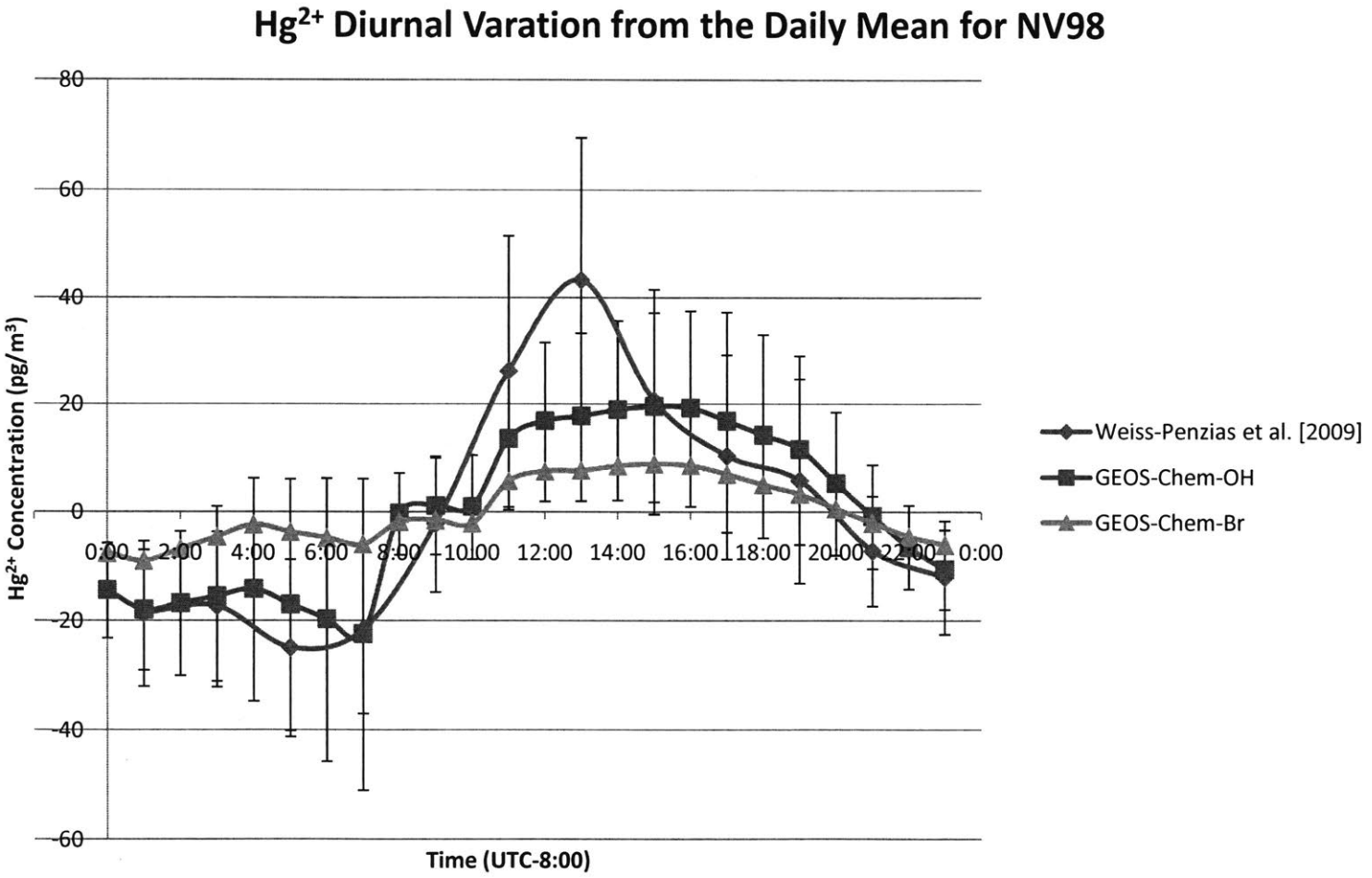

Hg^{2+} Diurnal Variation from the Daily Mean for NV98. The blue –diamond line indicates the *Weiss-Penzias et al.* [2009] data. The green triangle line is the GEOS-Chem Br model run. The red square line is the GEOS-Chem OH model run. The error bars are ±1 standard deviation. Note that none of the model runs have a high enough diurnal amplitude and that neither model runs peak during the correct time of day.

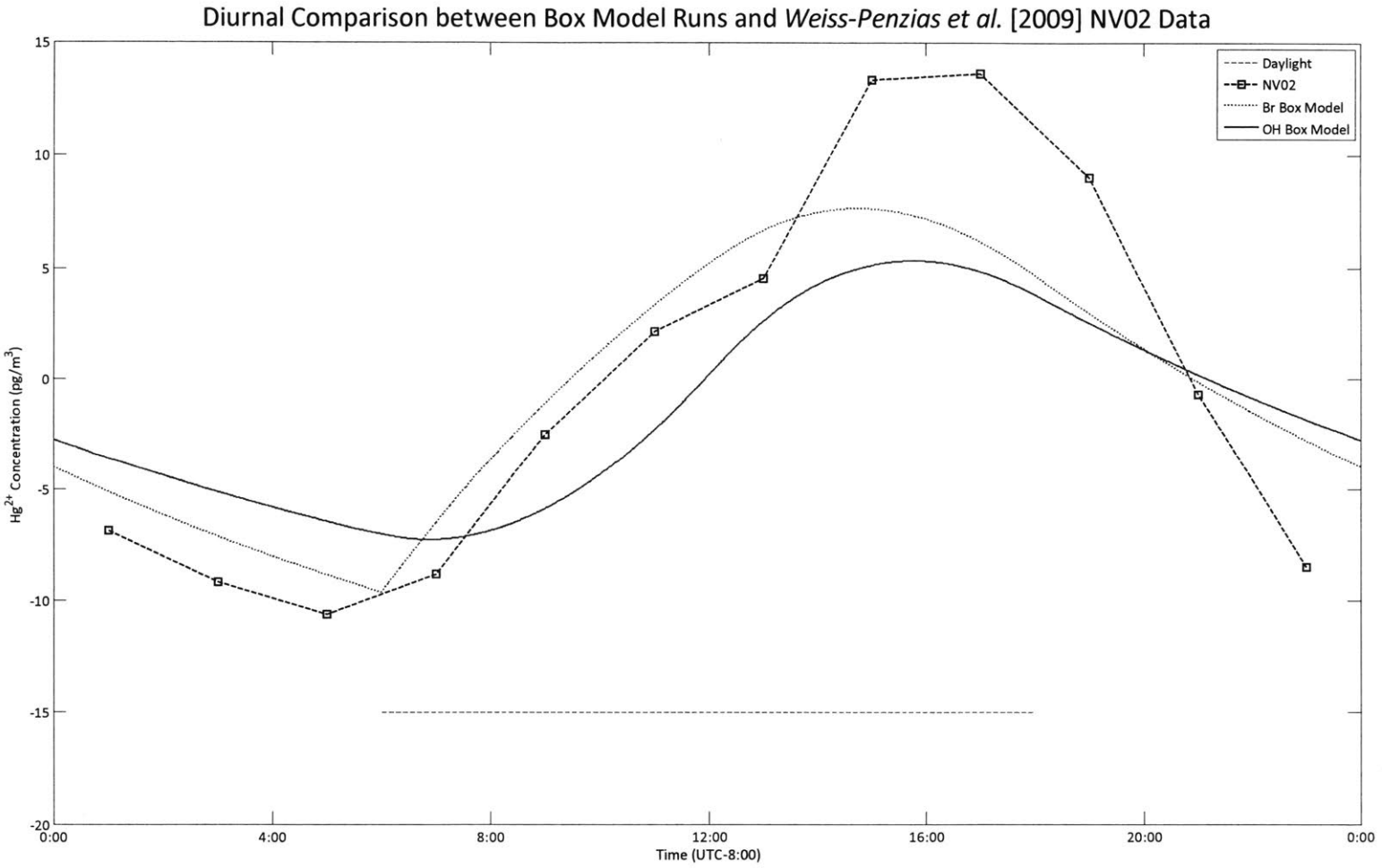

Diurnal Comparison between Box Model Runs and *Weiss-Penzias et al.* [2009] NV02 Data. The blue square dashed line shows the NV02 variations from the mean. The red dashed line shows the Br box model run. The green solid line shows the OH box model run. The orange dashed line indicates daylight hours. This graph shows variations from the mean. Note that the initial box model runs are closer to the DRI data than for the other sites. This is due to the fact that the diurnal amplitude for NV02 was smaller than for the other sites. This graph shows hourly variations from the daily mean.

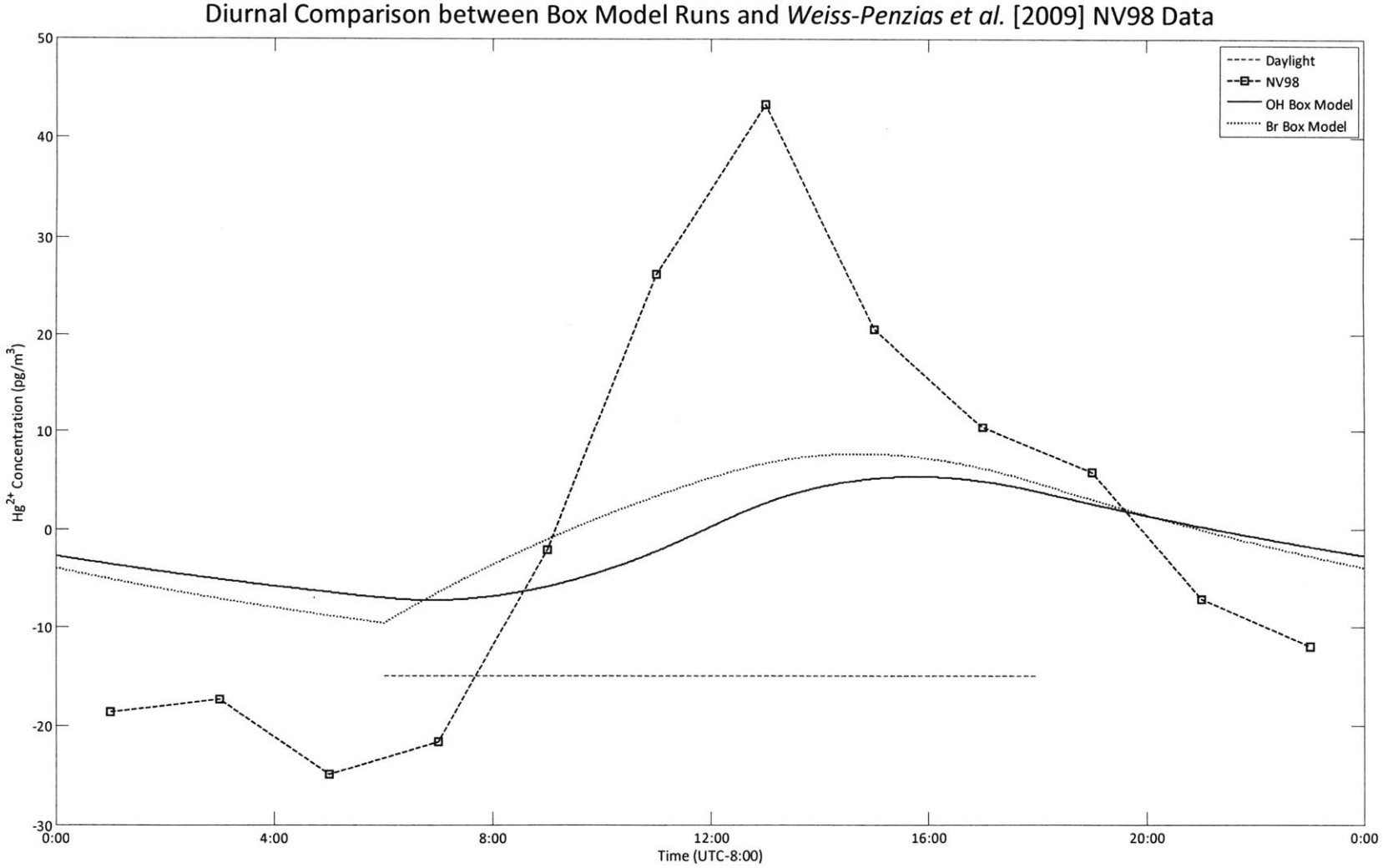

Diurnal Comparison between Box Model Runs and *Weiss-Penzias et al.* [2009] NV98 Data. The blue square dashed line shows the NV98 variations from the mean. The red dashed line shows the Br box model run. The green solid line shows the OH box model run. The orange dashed line indicates daylight hours. This graph shows hourly variations from the daily mean.

BIBLIOGRAPHY

"Air Pollution Prevention and Control." Title 42 *U.S. Code*, Sec. 7401-7671(q). 2008 ed., 5673-5965. http://www.gpo.gov/fdsys/pkg/USCODE-2008-title42/pdf/USCODE-2008-title42-chap85.pdf.

Bey I., D.J. Jacob, R.M. Yantosca, J.A. Logan, B. Field, A.M. Fiore, Q. Li, H.Y. Liu, L.J. Mickley, and M.G. Schultz (2001), Global modeling of tropospheric chemistry with assimilated meteorology: Model description and evaluation, *J. Geophys. Res., 106,* 23,073-23,095.

Buxton, J.T., J.C. Hewitt, R.H. Gadsen, and G.B. Bradham (1965), Metallic Mercury Embolism, *JAMA, 193*(7), 573-575, doi:10.1001/jama.1965.03090070023006.

Calvert, J.G. and S.E. Lindberg (2005), Mechanisms of mercury removal by O_3 and OH in the atmosphere, *Atmos. Environ., 39,* 3355-3367.

Carpi A., and S.E. Lindberg (1998), Application of a Teflon™ dynamic flux chamber for quantifying soil mercury flux: tests and results over background soil, *Atmos. Environ., 29,* 267-282.

Castoldi, A.F., T. Coccini, S. Ceccatelli, and L. Manzo (2001), Neurotoxicity and molecular effects of methylmercury, *Brain Research Bulletin, 55*(2), 197-203, doi:10.1016/S0361-9230(01)00458-0.

Coolbaugh, M.F., M.S. Gustin, and J.J. Rytuba (2002), Annual emissions of mercury to the atmosphere fro m natural sources in Nevada and California, *Environ. Geol., 42,* 338-349, doi:10.1007/s00254-002-0557-4.

Engle, M.A., M.T. Tate, D.P. Krabbenhoft, J.J. Schauer, A. Kolker, J.B. Shanley, and M.H. Bothner (2010), Comparison of atmospheric mercury speciation and deposition at nine sites across central and eastern North America, *J. Geophys. Res., 115,* D18306, doi:10.1029/2010JD014064.

Environmental Protection Agency, Mercury Study Report to Congress, *EPA-452/R-97-004*, U.S. Govt. Print. Off., Washington, D.C., 1997.

Faïn, X., D. Obrist, A.G. Hallar, I. Mccubbin, and T. Rahn (2009), High levels of reactive gaseous mercury observed at high elevation research laboratory in the Rocky Mountains, *Atmos. Chem. Phys. 9,* 8049-8060.

Fritsche, J., D. Obrist, and C. Alewell (2008), Evidence of microbial control of Hg^0 emissions from uncontaminated terrestrial soils, *J. Plant Nutr. Soil Sci., 171,* 200-209.

Garside, M.C., and J.H. Schilling (1979), Thermal wasters of Nevada, *Nev. Bur. Mines Geol. Bull., 91,* 163 pp.

Guentzel, J.L., W.M. Landing, G.A. Gill, and C.D. Pollman (2001), Processes influencing rainfall deposition of mercury in Florida, *Environ. Sci. Technol., 35,* 863-873.

Gustin, M.S. (2003) Are mercury emissions from geologic sources significant? A status report, *Sci. Total Environ., 304,* 153-167.

Gustin, M. and D. Jaffe (2010), Reducing the uncertainty in measurement and understanding of mercury in the atmosphere, *Environ. Sci. Technol, 44,* 2222-2227.

Gustin, M.S., M.F. Coolbaugh, M.A. Engle, B.C. Fitzgerald, R.E. Keislar, S.E. Lindberg, D.M. Nacht, J. Quashnick, J.J. Rytuba, C. Sladek, H. Zhang, and R.E. Zehner (2003), Atmospheric mercury emissions from mine wastes and surrounding geologically enriched terrains, *Environ. Geol., 43,* 339-351, doi:10.1007/s00254-002-0640-z.

Hall, B. (1995), The gas phase oxidation of elemental mercury by ozone, *Water Air Soil Pollut., 80,* 301-315.

He, Y., A.H. Monahan, C.G. Jones, A. dai, S. Biner, D. Caya, and K. Winger (2010), Probability distributions of land surface speeds over North America, *J. Geophys. Res. 115,* D04103, doi:10.1029/2008JD010708.

Holmes, C.D., D.J. Jacob, and X. Yang (2006), Global lifetime of elemental mercury against oxidation by atomic bromine in the free troposphere.

Holmes, C.D., D.J. Jacob, R.P. Mason, and D.A. Jaffe (2009), Sources and deposition of reactive gaseous mercury in the marine atmosphere, *Atmos. Environ.* 43:2278-2285.

Holmes, C.D., D.J. Jacob, E.S. Corbitt, J. Mao, X. Yang, R. Talbot, and F. Slemr (2010), Global atmospheric model for mercury including oxidation by bromine atoms, *Atmos. Chem. Phys.* 10:12037-12057.

Jacob, Daniel J. (1999), *Introduction to Atmospheric Chemistry,* Princeton Univ. Press, New Jersey.

Jaffe, D., E. Prestbo, P. Swartzendruber, P. Weiss-Penzias, S. Kato, A. Takami, S. Hatakeyama, and Y. Kajii (2005), Export of atmospheric mercury from Asia, *Atmos. Environ., 39,* 3029-3038.

Kerper, L.E., N. Ballatori, and T.W. Clarkson (1992), Methylmercury transport across the blood-brain barrier by an amino acid carrier, *Am. J. Physiol, 262*(5), R761-R765.

Landis, M.S., R.K. Stevens, F. Schaedlich, and E.M. Prestbo (2002) Development and characterization of an annular denuder methologody for the measurement of divalent inorganic reactive gaseous mercury in ambient air, *Environ. Sci. Technol., 36,* 3000-3009.

Laurier, F., and R.P. Mason (2007), Mercury concentration and speciation in the coastal and open ocean boundary layer, *J. Geophys. Res., 112*(D6), D06302, doi:10.1029/2006JD007320.

Laurier, F.J.G., R.P. Mason, L. Whalin, and S. Kato (2003), Reactive gaseous mercury formation in the North Pacific Ocean's marine boundary layer: A potential role of halogen chemistry, *J. Geophys. Res., 108*(D17), 4529, doi:10.1029/2003JD003625.

Lin, C.-J., and S.O. Pehkonen (1999), The chemistry of atmospheric mercury: A review, *Atmos. Environ., 33*, 2067-2079.

Lin, C.-J., P. Pongprueska, S.E. Lindberg, S.O. Pehkonen, D. Byun, and C. Jang (2006), Scientific uncertainties in atmospheric mercury models I; model science evaluation, *Atmos. Environ.* 40:2911-2928.

Lindberg, S.E. and W.J. Stratton (1998), Atmospheric mercury speciation: Concentrations and behavior of reactive gaseous mercury in ambient air, *Environ. Sci. Technol., 32,* 49-57.

Lindberg, S., R. Bullock, R. Ebinghaus, D. Engstrom, X. Feng, W. Fitzgerald, N. Pirrone, E. Prestbo, and C. Seigneur (2007), A synthesis of progress and uncertainties in attributing the sources of mercury in deposition, *Royal Swedish Academy of Science, 36*(1), 19-33.

Lyman, S.N., and M.S. Gustin (2007), Speciation of atmospheric mercury at two sites in northern Nevada, USA, *Atmos. Environ., 42,* 927-939, doi:10.1016/j.atmosenv.2007.10.012.

"National Emission Standards for Hazardous Air Pollutants from Coal- and Oil-Fired Electric Utility Steam Generating Units and Standards of Performance for Fossil-Fuel-Fired Electric Utility, Industrial-Commercial-Institutional, and Small Industrial-Commercial-Institutional Steam Generating Units." Title 40 *Code of Federal Regulations,* Pts. 60 and 63. 2011 ed.

New Jersey v. Environmental Protection Agency, 517 F.3d 574 (D.C. Cir. 2008).

Mason, R.P. and G.-R. Sheu (2002), Role of the ocean in the global mercury cycle, *Glob.Biogeochem. Cycles, 16*(4), 1093, doi:10.1029/2001GB001440.

Mason, R.P., W.F. Fitzgerald, and F.M.M. Morel (1994), The biogeochemical cycling of elemental mercury: anthropogenic influences, *Geochimica et Cosmochimica Acta* 54(15):3191-3198.

McLinden, C.A., C.S. Haley, N.D. Lloyd, F. Hendrick, A. Rozanov, B.-M. Sinnhuber, F. Goutail, D.A. Degenstein, E.J. Llewellyn, C.E. Sioris, M. Van Roozendael, J.P. Pommereau, W. Lotz, and J.P. Burrows (2010), Odin/OSIRIS observations of stratospheric BrO: Retrieval methodology, climatology, and inferred Br_y, *J. Geophys. Res., 115,* D15308, doi:10.1029/2009JD012488.

Mergler D., H.A. Anderson, L.H.M. Chan, K.R. Mahaffey, M. Murray, M. Sakamoto, and A.H. Stern (2007), Methylmercury exposure and health effects in humans: a worldwide concern, *Ambio: A J. Hum. Environ.,* 36:3-11.

Pacyna, J., S. Wilson, F. Steenhuisen, and E. Pacyna (2005), *Partially distributed inventories of global anthropogenic emissions of mercury to the atmosphere.* http://www.amao.no/Resources/HgEmissions/HgInventoryData.html.

Pal, B., and P.A. Ariya (2004a), Gas-phase HO-initiated reactions of elemental mercury: Kinetics, product studies, and atmospheric implications, *Environ. Sci. Technol., 38,* 5555-5566.

Pal, B., and P.A. Ariya (2004b), Studies of ozone initiated reactions of gaseous mercury: Kinetics, product studies, and atmospheric implications, *Phys. Chem. Chem. Phys., 6,* 572-579.

Park, R.J., D.J. Jacob, B.D. Field, R.M. Yantosca, and M. Chin (2004), Natural and trans-boundary pollution influences on sulfate-nitrate-ammonium aerosols in the United States: Implications for policy, *J. Geophys. Res., 109,* D15204. doi:10.1029/2003JD004473.

Perry, E., S.A. Norton, N.C. Kamman, P.M. Lorey, and C.T. Driscoll (2005), Deconstruction of historic mercury accumulation in lake sediments, northeastern United States, *Ecotoxicology, 14,* 85-99

Pirrone, N., I. Allegrini, G.J. Keeler, J.O. Nriagu, R. Rossman, and J.A. Robbins (1998), Historical atmospheric mercury emissions and depositions in North America compared to mercury accumulations in sedimentary records, *Atmos. Environ., 32*(5), 929-940.

Pleijel, K. and J. Munthe (1995), Modeling the atmospheric mercury cycle-chemistry in fog droplets, *Atmos. Environ., 29*(12), 1441-1457.

Ravichandran, M. (2004), Interactions between mercury and dissolved organic matter-a review, *Chemosphere, 55,* 319-331.

Seigneur, C. and K. Lohman (2008), Effect of bromine chemistry on the atmospheric mercury cycle, *J. Geophys. Res. 113*, D23309, doi:10.1029/2008JD010262.

Seinfeld, J.H. and S.N. Pandis (1998), *Atmospheric Chemistry and Physics: From Air Pollution to Climate Change,* John Wiley & Sons, New York.
Selin, N.E. (2009), Global biogeochemical cycling of mercury: a review, *Annu. Rev. Environ. Resour.* 34:43-63.

Selin, N.E. and D.J. Jacob (2008), Seasonal and spatial patterns of mercury wet deposition in the United States: Constraints on the contribution from North American anthropogenic sources, *Atmos. Environ., 42,* 5193-5204.

Selin, N.E., D. J. Jacob, R.J. Park, R.M. Yantosca, S. Strode, L. Jaeglé, and D.A. Jaffe (2007), Chemical cycling and deposition of atmospheric mercury: Global constraints from observations, *J. Geophys. Res., 112,* D02308, doi:10.1029/2006JD007450.

Selin, N.E., D.J. Jacob, R. M. Yantosca, S. Strode, L. Jaelgé, and E.M. Sunderland (2008), Global 3-D land-ocean-atmosphere model for mercury: Present-day versus preindustrial cycles

and anthropogenic enrichment factors for deposition, *Global Biogeochem. Cycles, 22,* GB2011, doi:10.1029/2007GB003040.

Slemr, F., G. Schuster, and W. Seiler (1985), Distribution, speciation, and budget of atmospheric mercury, *J. of Atmos. Chem, 3,* 407-434.

Soerensen, A.L., E.M. Sunderland, C.D. Holmes, D.J. Jacob, R.M. Yantosca, H. Skov, J.H. Christensen, S.A. Strode, and R.P. Mason (2010), An improved global model for air-sea exchange of mercury: High concentrations over the North Atlantic, *Environ. Sci. Technol., 44,* 8574-8580.

"Standards of Performance for New and Existing Stationary Sources: Electronic Utility Steam Generating Units." Title 40 *Code of Federal Regulations*, Pts. 60, 63, 72, and 75. 2005 ed.

Strode, S.A., L. Jaegle, N.E. Selin, D.J. Jacob, R.J. Park, R.M. Yantosca, R.P Mason, and F. Slemr (2007), Air-sea exchange in the global mercury cycle, *Glob. Bio-geochem. Cycles, 21,* GB4022.

Strode, S., L. Jaegle, and N.E. Selin (2009), Impact of mercury emissions from historical gold and silver mining: Global modeling, *Atmos. Environ., 43,* 2012-2017.

Stull, R.B. (1988), *An Introduction to Boundary Layer Meterology,* Kluwer Academic, Dordrecht.

Swain, E.B., D.R. Engstrom, M.E. Brigham, T.A. Henning, and P.L. Brezonik (1992), Increasing rates of atmospheric mercury deposition in midcontinental North-America, *Science, 257*(5071), 784-787.

Swartzendruber, P.C., D.A. Jaffe, E.M. Prestbo, P. Weiss-Penzias, N.E. Selin, R. Park, D.J. Jacob, S. Strode, and L. Jaeglé (2006), Observations of reactive gaseous mercury in the free troposphere at the Mount Bachelor Observatory, *J. Geophys. Res. 111,* D24301, doi:10.1029/2006JD007415.

Ullrich, S., T. Tanton, and S. Abdrashitova (2001), Mercury in the aquatic environment: A review of factors affecting methylation," *Critical Reviews in Environmental Science and Technology, 31*(3), doi:10.1080/20016491089226

Varekamp, J.C. and P.R. Buseck (1986), Global mercury flux from volcanic and geothermal sources, *Appl. Geochem., 1,* 65-73.

Vo, A.-T.E., M.S. Bank, J.P. Shine, and S.V. Edwards (2011), Temporal increase in organic mercury in an endangered pelagic seabird assessed by century-old museum specimens, *Proc. Natl Acad. Sci. USA,* doi:10.1073/pnas.1013865108.

Wang, Z. and S.O. Pehkonen (2004), Oxidation of elemental mercury by aqueous bromine: atmospheric implications, *Atmos. Environ., 38,* 3675-3688.

Weiss-Penzias, P., D. Jaffe, P. Swartzendruber, W. Hafner, D. Chand, and E. Prestbo (2007), Quantifying Asian and biomass burning sources of mercury using the Hg/CO ratio in pollution plumes observed at the Mount Bachelor Observatory, *Atmos. Environ., 36,* 4366-4379.

Weiss-Penzias, P., M.S. Gustin, and S.N. Lyman (2009), Observations of speciated atmospheric mercury at three sites in Nevada: evidence for a free tropospheric source of reactive gaseous mercury, *J. Geophys. Res. 114*, D14302, doi:10.1029/2008JD011607.

Wolfe, M.F., S. Schwarzbach, and R.A. Sulaiman (1998), Effects of mercury of wildlife: a comprehensive review, *Environ. Toxicol. Chem., 17,* 146-160.

World Health Organization (1990), Methylmercury. Environmental Health Criteria 101. World Health Organization, International Programme on Chemical Safety, Geneva, Switzerland.

Zhang, L., L.P. Wright, and P. Blanchard (2009), A review of current knowledge concerning dry deposition of atmospheric mercury, *Atmos. Environ., 43*, 5853-5864.